

STERIC EFFECTS IN INTERACTION BETWEEN  
TRANSMEMBRANE PROTEINS AND PHOSPHOLIPIDS

A Dissertation

Presented to the Faculty of the Graduate School

of Cornell University

in Partial Fulfillment of the Requirements for the Degree of

Doctor of Philosophy

by

Khatuna Kachlishvili

May 2011

© 2011 Khatuna Kachlishvili

# STERIC EFFECTS IN INTERACTION BETWEEN TRANSMEMBRANE PROTEINS AND PHOSPHOLIPIDS

Khatuna Kachlishvili, Ph.D.

Cornell University 2011

The methylene-interrupted, all-cis (*Z*) bond configuration is overwhelmingly favored in polyunsaturated fatty acids (PUFA) of vertebrate membranes, particularly the highly unsaturated membranes of electrically-active neural tissue. The hypothesis that hexaene and pentaene homoallylic groups are sterically allowed to follow the groove of a transmembrane  $\alpha$ -helix from bovine rhodopsin using energy minimization (EM) and molecular dynamics (MD) simulations with the GROMOS96 force field was investigated. Docosahexaenoic acid (22:6n-3) and docosapentaenoic acid (22:5n-6) were configured along arbitrary, mid-, top-helix paths along helix 2, with the doubly allylic hydrogens directed inward and the ethylenic hydrogens directed out of the helix. It was shown, by performing EM and MD simulations for 22:6n-3 and 22:5n-6, that the rotationally constrained homoallylic regions are more stably contained within the groove than saturated regions. The analyses of the initial conformations of 22:6n-3 in phosphatidylcholine-22:6n-3/34:5n-3 and 22:5n-6 in phosphatidylcholine-22:5n-6/34:5n-3, and of conformations of 22:6n-3 in phosphatidylcholine-22:6n-3/34:5n-3

obtained after EM showed that the homoallylic regions fit loosely within the groove while the saturated regions are much closer to the groove boundary. Calculations using a configuration with phosphatidylcholine-22:6n-3/34:5n-3 showed that the 22:6n-3 chain can follow the groove nearest a membrane-water interface, while the homoallylic region of the very long chain 34:5n-3 can follow the groove nearer the membrane center, tethered by its extended saturated region. These results illustrate that the homoallylic polyunsaturated fatty acid motif is not sterically restricted from occupying the groove of a transmembrane  $\alpha$ -helix and provide a testable prediction. The biophysical stability and properties conferred by this configuration was speculated.

## **BIOGRAPHICAL SKETCH**

Khatuna Kachlishvili was born in Tbilisi, Georgia on April 3, 1965, the second child of Zaur Kachlishvili and Liana Shavadze. Khatuna grew up in Tbilisi and graduated with a gold medal from Tbilisi High School specialized in Physics and Mathematics in 1982.

Because of her family (her grandparents, father, and brother were all physicists), Khatuna became interested in physics and mathematics before High School. However, Khatuna was also interested in a multitude of other subjects spanning from literature to classical music, and it was only until the last moment that she was sure of her choice of pursuing physics. In 1982, Khatuna started her undergraduate studies at Tbilisi State University majoring in Physics. She graduated with honors from Tbilisi State University in 1987, receiving a Master of Science degree in Physics with specialization in Solid State Physics (advisor: Dr. Victor Bonch-Bruevich). During these years, she also took classes in screenwriting at the Department of Cinematography at Tbilisi State University.

In 1987, Khatuna entered Tbilisi State University as a graduate student to continue her research on the physics of semiconductors, which she had started in her undergraduate years. The majority of her research was performed at the Department of Physics in Moscow State University. Unfortunately, because of the tense political

and economical situation in Georgia, she was unable to defend her PhD thesis. Instead, she, with her husband and two sons immigrated to New Zealand.

In New Zealand Khatuna decided to take a break from Science. She was mainly busy with raising her children, and in her spare time she composed music, sang at concerts, and learned English.

In 2004, Khatuna resumed her scientific career as a graduate student at the University of Nevada – Reno, and then at Cornell University. Khatuna did her research in biophysical chemistry at the laboratory of Dr. J. Thomas Brenna at Cornell University from the fall of 2007 to the fall of 2010. She successfully defended her thesis in November 2010.

## ACKNOWLEDGEMENTS

First, I would like to thank my advisor, Dr. J. Thomas Brenna, for accepting me in his Lab, for his research ideas, and his guidance on my studies.

I am very grateful to Dr. Harold Scheraga for allowing me to use his cluster for my computations, his advice and help.

Thanks to Dr. Jack Freed, the member of my thesis committee, for his advice and careful reading of my thesis.

I am grateful to my parents for all their support during the many years of my education.

Finally, I would like to thank my family: my sons, Luka and Nika, for their support, understanding, love and patience during all these years; and my husband, Gia, for his tremendous help with my research, personal encouragement, and patience.



2.3. Results	32
2.3.1. DHA-helix vs DPAn-6-helix	35
2.3.2. Highly unsaturated homoallylic hydrocarbons may form a secondary helix in the groove of transmembrane protein $\alpha$ -helices	42
2.4. Discussion	58
2.5. Conclusions	60
References	63

## LIST OF FIGURES

1.1	Cell membrane	2
1.2	The seven-transmembrane $\alpha$ -helix structure of a G-protein-coupled receptor	4
1.3	Ribbon drawings of rhodopsin. (A) Parallel to the plane of the membrane (stereoview). A view into the membrane plane is seen from the cytoplasmic (B) and intradiscal side (C) of the membrane	6
1.4	Scheme of glycerophospholipids	10
1.5	Subgroups of Glycerophospholipids	12
1.6	Saturated fatty acids	14
1.7	Monounsaturated fatty acids	16
1.8	Polyunsaturated fatty acids	18
1.9	Docosahexaenoic acid	20
1.10	Phospholipid bilayer	21
2.1	22:6n-3 [in space-filling (a) and stick (b) models], 22:5n-3 [upper in panel (c)] and 22:5n-6 [lower in panel (c)] can assume a helical path that can follow the path of a transmembrane $\alpha$ -helix. The atoms in red correspond to oxygens	34
2.2	Proposed conformations of initial structure for DHA (a) and DPAn-6 (b) along with $\alpha$ -helix	37
2.3	Initial (a,d), after minimization (b,e) and restricted molecular	

	dynamics (c,f) positions of DHA and DPAn-6, respectively, wrapped in the middle of helix. The carbon chains of DHA and DPAn-6 are illustrated in cyan and grey color, respectively	39
2.4	Initial (a,d), after minimization (b,e) and restricted molecular dynamics (c,f) positions of DHA and DPAn-6, respectively, wrapped on the top of helix. The carbon chains of DHA and DPAn-6 are illustrated in grey color	40
2.5	DHA and DPAn-6 after minimization (a,c) and restricted molecular dynamics (b,d), respectively	41
2.6	Initial structure of PC-22:6-34:5 (a) and PC-22:5-34:5 (b) docked at the end of helix 2 of bovine rhodopsin	44
2.7	PC-22:6-34:5 (a) and PC-22:5-34:5 (b) and $\alpha$ -helix	46
2.8	PC-22:6-34:5 and helix (a) and PC-22:5-34:5 and helix (b). The saturated regions of 22:6n-3 and 22:5n-6 are in cyan color, and hydrogen atoms are in yellow color	47
2.9	The distance between the surfaces of N MET and N GLN is 3.413Å. The cyan color atoms are N's of Methionine and Glutamine. They are shown in spacefill models	48
2.10	PC-22:6-34:5 and helix (a, c) and PC-22:5-34:5 and helix (b, d). Nitrogen atoms are in cyan color, Hydrogen atoms are in yellow color	50
2.11	PC-22:6-34:5 and helix after minimization	52
2.12	Expanded view of the ethylenic hydrogen (in green) on C20 of 22:6n-3, showing hard sphere distances between the closest helix atoms (in red), both nitrogens	53
2.13	The first doubly allylic hydrogens from the methyl end are shown in	

a spacefill model. They belong to 22:6 of PC226345( $\omega$ 3) and are shown in blue color. The yellow-colored atoms belong to the second helix of rhodopsin

55

2.14 Space-filling energy-minimized model showing two opposing

views of the homoallylic chains (blue) buried to the  $\alpha$ -helix (red).

Left: View showing entry of the homoallylic chains from the glycerol backbone. Right: The 22:6 terminal methyl is buried within the groove of the  $\alpha$ -helix and covered by a TRP residue, while the terminal region of 34:5 extends out of the groove

57

## LIST OF TABLES

- 2.1 The distances between the atoms (in yellow) of the groove of  $\alpha$ -helix in the vicinity of C18 56

# Chapter 1

## Introduction

### 1.1. Cell membranes

The biological membranes, located around the cells, are called cell membranes. These cell membranes have many important functions that are crucial for life. They have different functions in different parts of the cell.

Cell membranes separate the inside and the outside environments of the cell. Cell membranes form a barrier in which the chemical environments inside and outside the barrier are different. Without the barrier cell membranes, there would be no control with the specific environments inside the cell.

Cell membranes are selectively-permeable, which means that they control what enters and exits the cell. Cell membranes do this work first, by choosing specific molecules and ions, and then giving them permission to go through the cell. In other words, with this function, the cell membranes control the changes inside the cell [1].

Another important function of the cell membrane is identification. Cell membranes differ from each other with their surfaces. The identification is a very important ability of the cell membranes which helps the cell identify another cell and

to react accordingly. Aside from above mentioned functions cell membranes are responsible for signaling and for energy conversion.

## 1.2. Constituents of the cell membranes

The cell membranes (Figure 1.1) have two main components: the amphipatic lipids and the embedded proteins. These proteins are integrated into cell membranes and are called transmembrane proteins. The transmembrane proteins can be alpha-helical or beta-barrels. All biological membranes have alpha-helical transmembrane proteins.

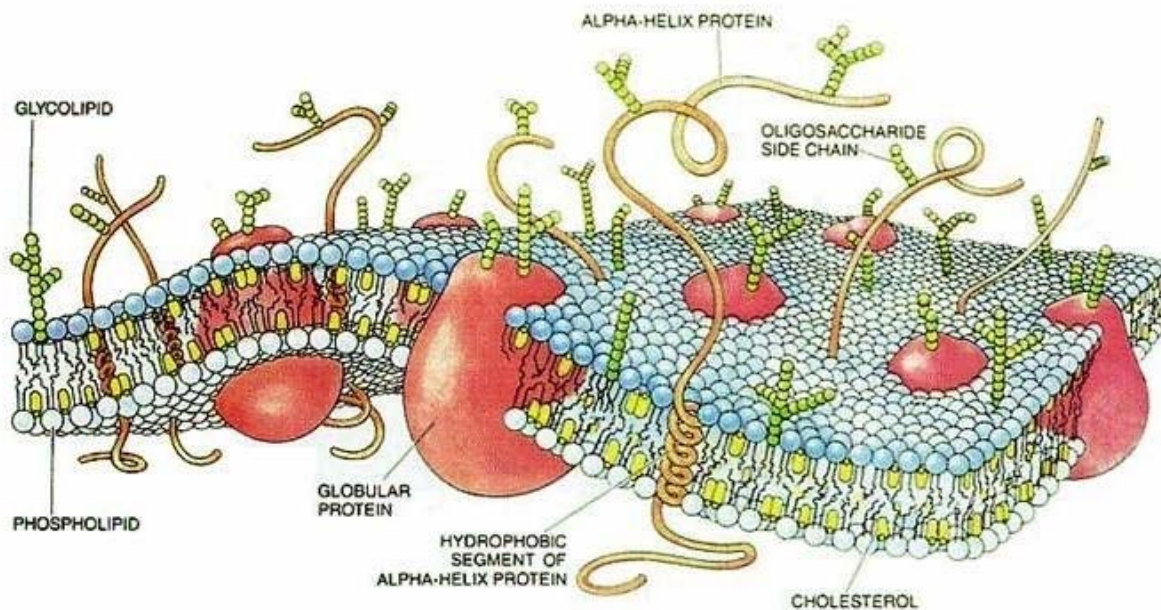


Figure 1.1: Cell membrane

### 1.3. Transmembrane proteins

G Protein-coupled receptors, also known as seven-transmembrane segment receptors (GPCRs or 7TM receptors) comprise the largest superfamily of proteins in the body (Figure 1.2). More than 1000 different GPCRs were identified since the first receptors have been cloned more than a decade ago [2]. The chemical diversity among the endogenous ligands is incomparable. They include glycoproteins, peptides, lipids, nucleotides, etc. The sensation of exogenous stimuli, such as light, taste, and odors, is mediated via this class of receptors. The extensive experimental work has uncovered multiple aspects of their function and challenged many traditional paradigms, insight into some of the most fundamental questions in the molecular function of the class of receptors was gained. It has been conceptualized that GPCRs are not simple “on/off” switches but highly dynamic structures that exist in equilibriums between active and inactive conformations [3].

Numerous schemes have been proposed for classification of GPCR superfamily. Finally, GPCR was grouped into six classes based on sequence homology and functional similarity [2, 4, 5]: class A (Rhodopsin-like), class B (Secretin receptor family), class C (Metabotropic glutamate/pheromone), class D (Fungal mating pheromone receptors), class E (Cyclic AMP receptors), class F (Frizzled/Smoothed).

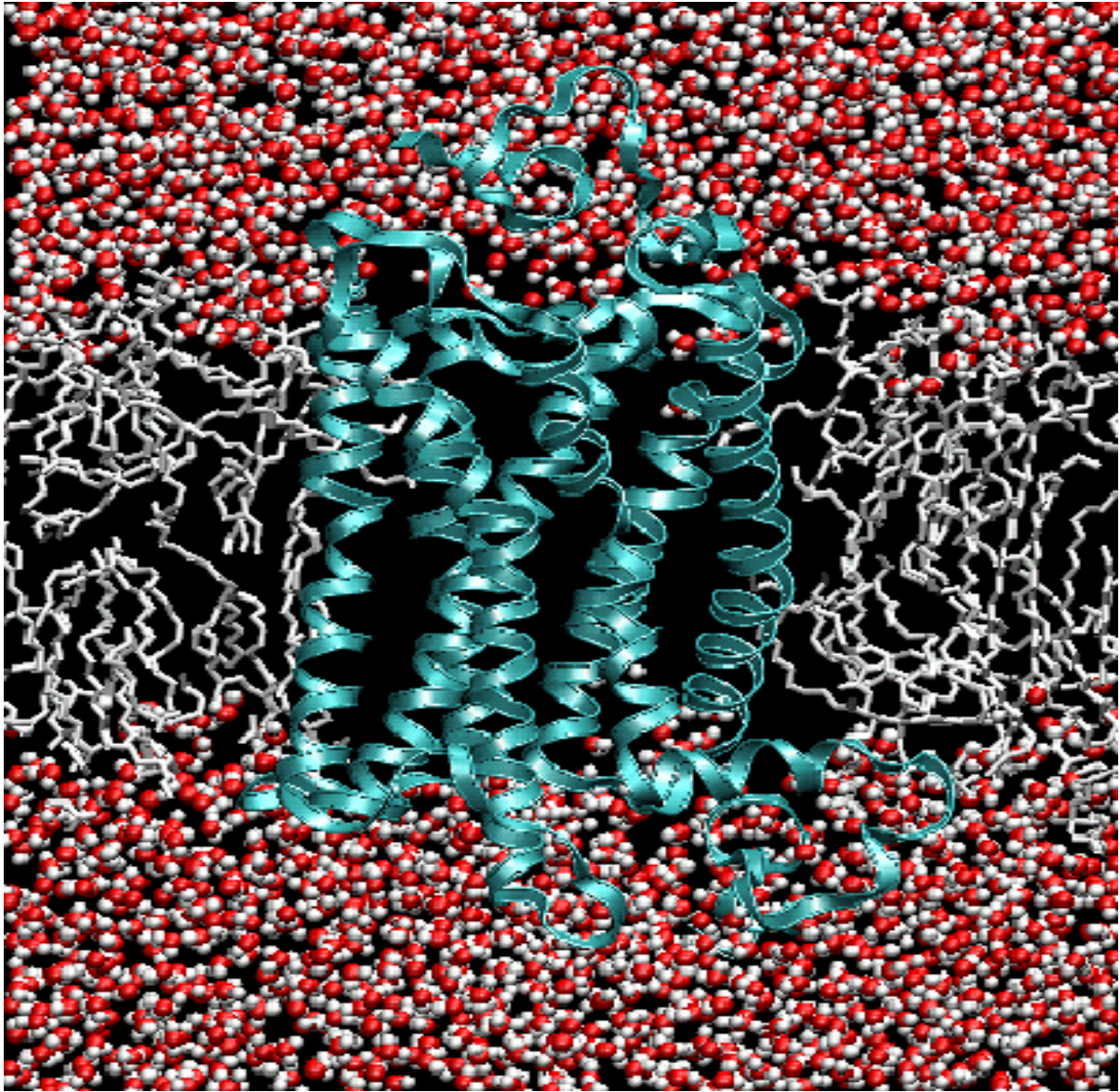


Figure 1.2: The seven-transmembrane  $\alpha$ -helix structure of a G-protein-coupled receptor.

Rhodopsins are the only member of the largest subfamily, constituting  $\sim 90\%$  of all G protein coupled receptors (GPCRs), for which a high-resolution crystal structure is available. Structure of rhodopsin was determined from diffraction data extending to 2.8 Å resolution [6], and uncovered a highly organized heptahelical transmembrane bundle with 11-*cis*-retinal as a key cofactor involved in maintaining rhodopsin in the ground state (Figure 1.3). Absorption of a photon by the 11-*cis*-retinal causes its isomerization to all-*trans*-retinal [7], leading to a conformational change of the protein moiety, including the cytoplasmic surface, where G-protein activation occurs. This conformational change leads to rhodopsin activation and signal transduction. Retinal's photoisomerization initiates a photocycle during which a thermally driven series of interconversions between rhodopsin's different conformational states happen. During the photocycle, the absorbed photon energy, initially stored internally in the form of a twisted structure of retinal, is used to induce conformational changes of retinal, of its binding pocket, and of the whole protein [8, 9]. The time-resolved UV/VIS spectroscopic measurements have shown that photobleaching of rhodopsin involves several intermediates and has more than one pathway [10, 11].

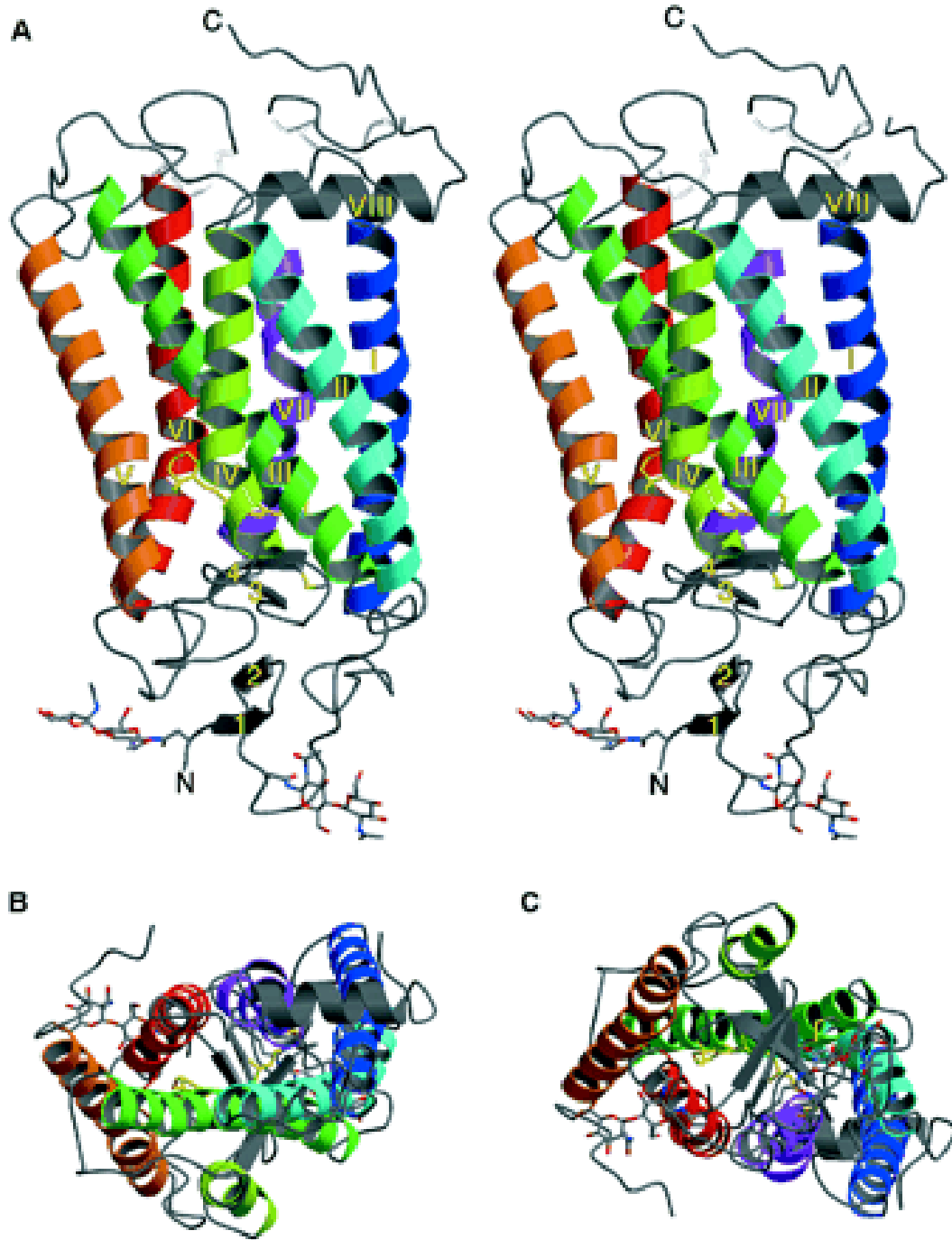


Figure 1.3: Ribbon drawings of rhodopsin. (A) Parallel to the plane of the membrane (stereoview). A view into the membrane plane is seen from the cytoplasmic (B) and intradiscal side (C) of the membrane.

The experiments have revealed many structural details of the receptor in the dark state [6, 12], such as all transmembrane helices are bent to different extents except for helix III, which is located in the middle of rhodopsin's helical bundle, the kinks, which are located near the retinal binding pocket at proline and glycine sites, may serve as molecular hinges that facilitate the conformational changes associated with the chromophore isomerization. However, there are some questions regarding the orientation of the rings and conformational changes during the photocycle which are still under debates, therefore, along with many experimental studies the molecular dynamics simulations, *ab initio* quantum mechanical calculations have been employed to solve those problems.

One of the first *ab initio* studies of the *in situ* isomerization dynamics of retinal in bacteriorhodopsin, a microbial retinal protein that functions as a light-driven proton pump in the purple membrane of *Halobacterium salinarum* [13] and is the most investigated member of family, revealed in complete molecular detail the photoisomerization process [14]. In particular, anomalously fast event in the primary process of bacteriorhodopsin's proton pump function was unveiled. Also, it was demonstrated that the protein plays essential role in the characteristic kinetics and high selectivity of the photoionization, i.e., the protein arrests inhomogeneous photoisomerization paths and funnels them into a single path which initiates the functional process. The multi-dimensional molecular motions, obtained by molecular

dynamics simulations, enhance the electronic transition from the excited state to the ground state and allow to identify the molecular origin of the dynamic spectral modulation phenomena observed in femtosecond spectroscopy [15-17].

By using the molecular dynamics simulations J. Saam et al. [18] studied the primary photoinduced events which prepare rhodopsin for major structural transformations achieved later in the photocycle.

Recently, B. Isin et al. [19] used molecular dynamics simulations to study functionally relevant conformational changes and signal transmission mechanisms involved in its photoactivation brought about through a *cis-trans* photoisomerization of retinal. Two highly stable regions in rhodopsin, one clustered near the chromophore and the other near the cytoplasmic ends of transmembrane helices 1, 2, and 7 were identified.

It is worthwhile to note that, the mutations of rhodopsin are the most common cause of autosomal-dominant retinitis pigmentosa (ADRP), which is a group of retinal degenerative diseases that are characterized by the loss of rod photoreceptor cells followed by cone degeneration [20, 21]. Patients with retinitis pigmentosa experience night blindness, the progressive loss of peripheral vision and eventually central vision as cone-cell viability is compromised by rod-cell death. Over 120 point mutations in rhodopsin have now been identified [22].

## 1.4. The lipids

Besides the transmembrane proteins the lipids are another important part of the cell membrane. Because of the amphipatic character of lipids, the lipid bilayer is formed inside the membrane. Lipids are naturally-occurring molecules, which are not soluble in water (generally) and are soluble in non-polar organic solvents such as chloroform, acetone, ether and benzene. The lipids can be extracted very easily from the proteins using these organic solvents. The groups of lipids are very large and they include molecules such as fat-soluble vitamins like A, D, E and K, fats, oils, sterols, cholesterol, phospholipids and others [23]. Lipids have an important role in human health and some of them are crucial for life, however, certain lipids like cholesterol, in abnormal amounts, can increase the risk factors for cardiovascular diseases. Lipids can be divided into these next categories: Fatty acyls, phospholipids, glycerolipids, sphingolipids, sterol lipids, prenol lipids, saccharolipids and polyketides. Each category includes different group of molecules. We are interested in lipids which are found in the cell membranes, these lipids are: phospholipids, glycolipids and cholesterol. Their amount in cell membranes depends on the type of the cell. Among these three lipids the phospholipids are the most abundant components of the cell membranes [24]. Their structure is based on the phosphate moiety.

## 1.5. The glycerophospholipids

The glycerophospholipids or phosphoglycerides, class of phospholipids, are glycerol- based and have three main components: diglyceride, a head group, and a phosphate group (Figure 1.4).

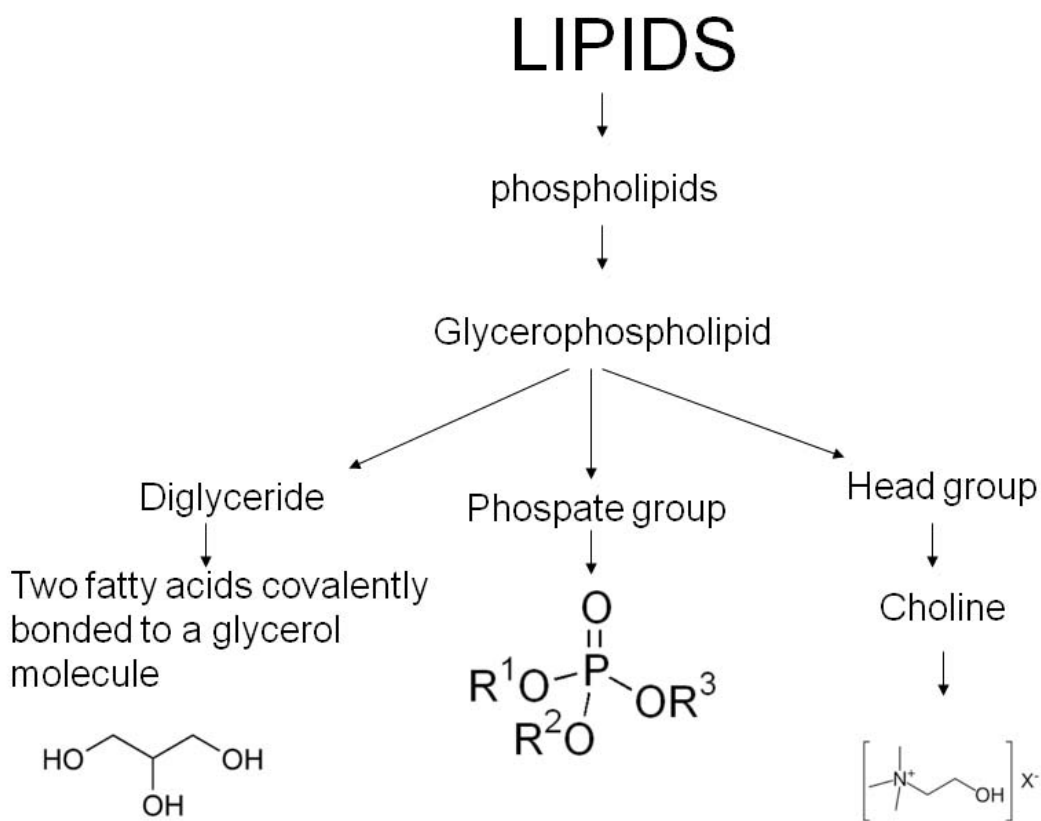


Figure 1.4: Scheme of glycerophospholipids.

The phospholipids that are sphingosine-based instead of glycerol, are another group of phospholipids and are called phosphosphingolipids. Among these two phospholipids, the glycerophospholipids are a major component in biological membranes and the key of the lipid bilayer. The subgroups of glycerophospholipids (Figure 1.5) differ with their headgroups and they are: PtdSer (Phosphatidylserine), PtdEtn (Phosphatidylethanolamine), PtdCho (Phosphatidylcholine) and PtdIns (Phosphatidylinositol) [23]. In general, all these glycerophospholipids have the same covalently bonded phosphate group with diglycerides by ester linkage and they differ with the head groups and correspondingly with their charges.

Among these glycerophospholipids the phosphatidylcholines have been studied intensively in this project, because they are the main components of biological membranes and the key components of lipid bilayer. The phosphatidylcholine contains three main parts: the diglyceride, where two fatty acids are covalently bonded to a glycerol molecule; the phosphate group and choline as a head group.

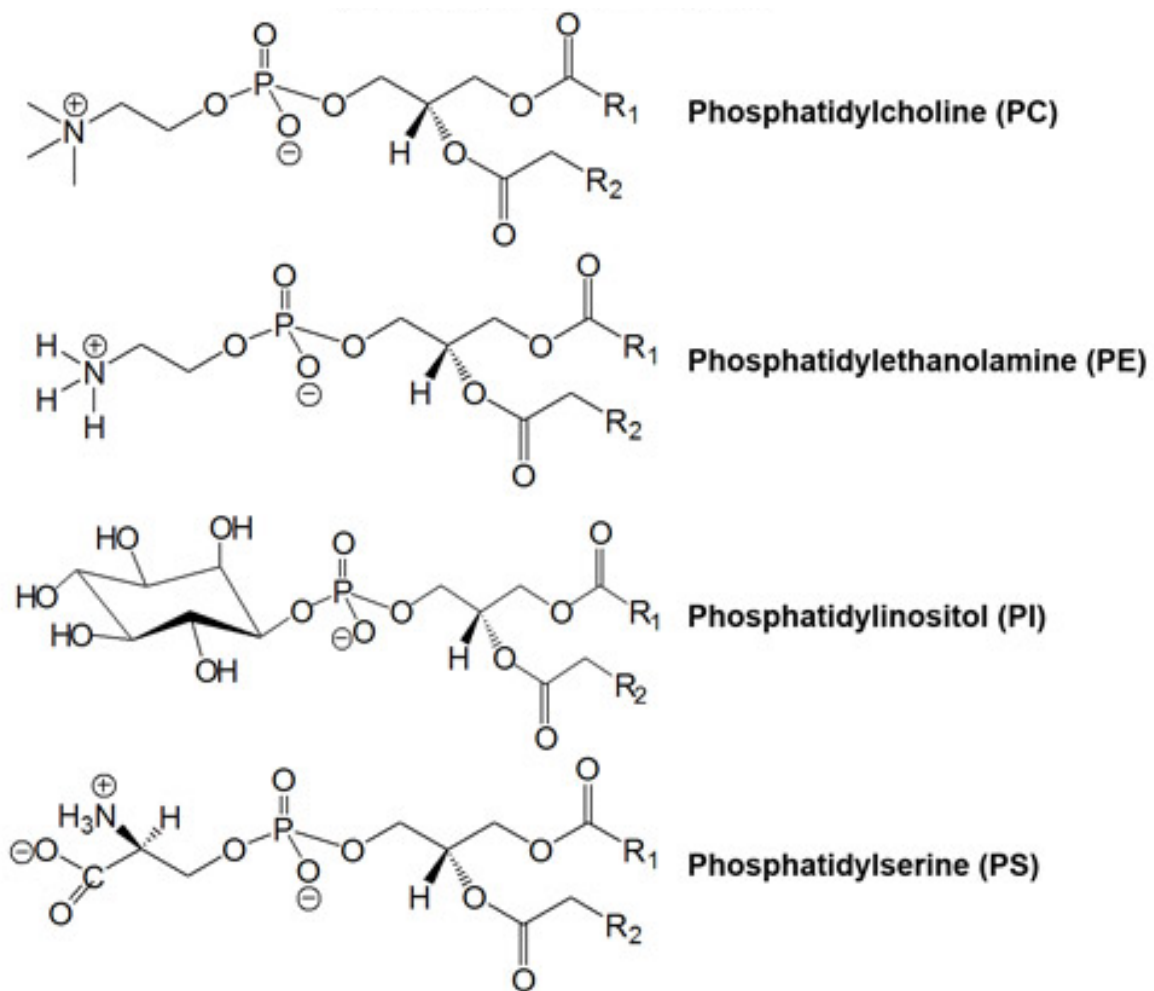


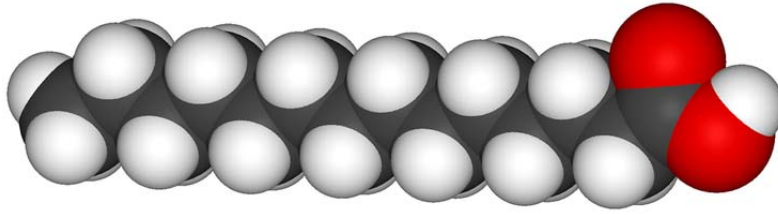
Figure 1.5: Subgroups of Glycerophospholipids

## 1.6. The fatty acids

In the phosphatidylcholines, like other phospholipids, the two fatty acids are covalently bonded with a glycerol backbone. Fatty acids are carboxylic acids with a long aliphatic (hydrocarbon) chain. In general, natural fatty acids have an even number of carbons. The fatty acids are produced when fats are broken down [25]. These acids are slightly soluble in water and they can be used for energy by most types of cells. The length of hydrocarbon chain may vary from 4 and can be more than 18 [26, 27]. Depending of the number of double bonds in an aliphatic chain, fatty acids can be divided as a monounsaturated (MUFA), polyunsaturated (PUFA), or saturated (SFA) fatty acids [28].

Saturated fatty acids do not contain any double bonds or other functional groups along the chain [Figure 1.6 (a, b)]. The SFAs, general formula of which is  $\text{CH}_3(\text{CH}_2)_n\text{COOH}$ , have commonly straight chains and the number of carbon atoms ranging from 4 to 30. The term "saturated" refers to hydrogen, in that all carbons (apart from the carboxylic acid [-COOH] group) contain as many hydrogens as possible. Because of the straight chains form, SFA can be packed together very tightly, allowing living organisms to store chemical energy very densely. The fatty tissues of animals contain large amounts of long-chain saturated fatty acids.

(a)



(b)

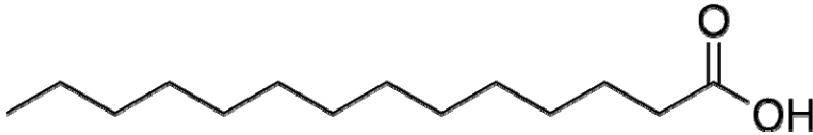
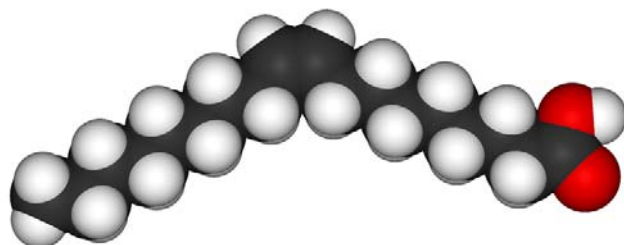


Figure 1.6: Saturated fatty acids

Monounsaturated normal fatty acids are widespread in the living world. The general chemical formula:  $\text{CH}_3(\text{CH}_2)_x\text{CH}=\text{CH}(\text{CH}_2)_y\text{COOH}$ . They have a single double bond in the fatty acid chain and all of the remainder of the carbon atoms in the chain are single-bonded. The most frequently number of carbon atoms is even, and the double bond can be placed at different positions. Depending on the stereoisomeric form in which the double bond exists MUFAs are either *cis*-monoenoic fatty acids or *trans*-monoenoic fatty acids. In other words, the hydrogen atoms in *cis*-

isomer are present on the same side of the double bond, whereas in the *trans* configuration they are on opposite sides. The *cis*-monoenoic fatty acids are more frequent in the nature than *trans*-isomer. The most common *cis*-monoenoic fatty acid is oleic acid ( $\text{CH}_3(\text{CH}_2)_7\text{CH}=\text{CH}(\text{CH}_2)_7\text{COOH}$ ) [Figure 1.7 (a, b)] found in various animal and vegetable sources such as olive oil, pecan and peanut oil, chicken and turkey fat, lard, etc. The *trans*-isomer of oleic acid - elaidic acid [Figure 1.7 (c, d)] is mainly found in hydrogenated vegetable oils and occurs in small amount in caprine and bovine milk.

(a)



(b)

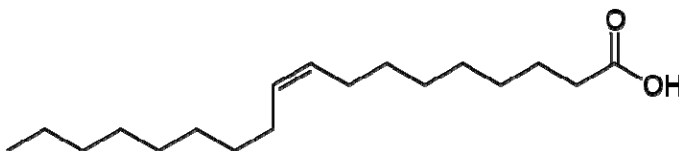
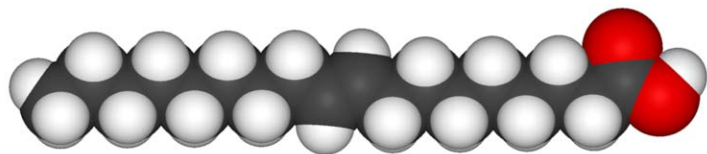


Figure 1.7 (Continued)

(c)



(d)

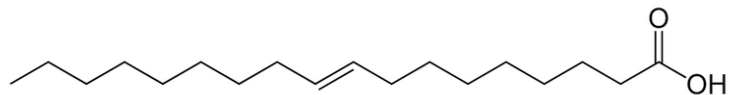


Figure 1.7: Monounsaturated fatty acids

Since our daily food contains both monounsaturated fatty acids and saturated fatty acids, the effect of MUFAa and SFAs on human health was extensively studied. In particular, their effect on cardiovascular disease (CVD) and coronary heart disease (CHD). Recent studies [29] showed the relation of *trans* MUFA to CVD risk.

Polyunsaturated fatty acids (PUFA) have two or more double bonds on their hydrocarbon chains. The double bonds are separated with a methylene group. In fatty acids, increasing the number of double bond results in the number of hydrogen atoms decreasing, which weakens the intermolecular forces and lowers the melting point.

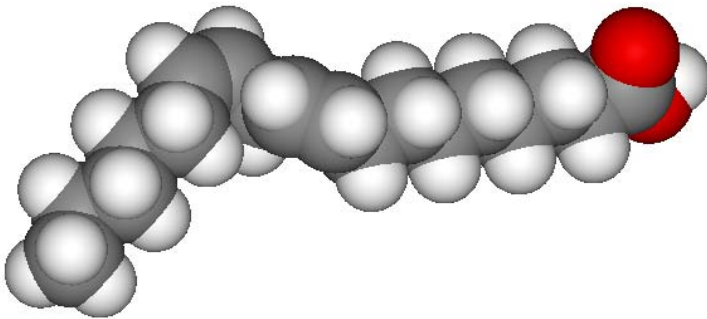
The fatty acids have a methyl group and carboxylic acid on their ends. Unsaturated fatty acids can be divided into three categories:  $\omega$ -3,  $\omega$ -6 and  $\omega$ -9 fatty acids depending on the location of first double bond from terminal methyl end. In  $\omega$ -3 fatty acids first double bond from terminal methyl end appears after three carbons, n-3 position, when in  $\omega$ -6 and  $\omega$ -9 only, correspondingly, after 6 and after 9 carbons from terminal methyl end appears the first double bonds.

Omega-3 fatty acids are essential fatty acids. The body cannot synthesize them, but humans can get omega-3 fatty acids through diet. Their health benefit is tremendous. Deficiency of omega-3 fatty acids can cause lot of health problems, like heart problem, memory problem, depression, fatigue and more. Omega-3 fatty acids can reduce inflammation, when some omega-6 fatty acids can promote inflammation. In human diet, it is very important to maintain a balance of omega-3 and omega-6 fatty acids.

Among omega fatty acids,  $\omega$ -6 fatty acid- Linoleic acid (LA, 18:2n-6) with 18 carbons and 2 double bonds [Figure 1.8 (a, b)], and  $\omega$ -3 fatty-acid Alpha-linolenic acid (ALA,

18:3n-3) with 18 carbons and 3 double bonds, are considered dietary essential short chain polyunsaturated fatty acids (AFA). The human body can't synthesize them, however they are helping to create long-chain polyunsaturated fatty acids (LCPUFA), like docosahexaenoic acid (DHA, 22:6n-3) with 22 carbons and 6 double bonds.

(a)



(b)

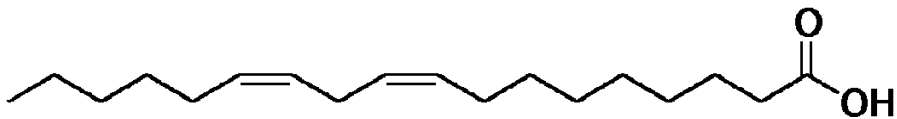


Figure 1.8: Polyunsaturated fatty acids

Omega-9 fatty acids can be produced by the human body and they are not essential for life. Because of these two reasons,  $\omega$ -9 fatty acids are not considered essential fatty acids.

### **1.7. Docosahexaenoic acid**

As mentioned above, the polyunsaturated fatty acids are a main component of cell membranes [30]. Among these fatty acids, the docosahexaenoic acid ( $\omega$ -3 fatty acid) (Figure 1.9) has a special role in human health. Docosahexaenoic acid is vital for the healthy functioning of the retina, the brain, the mitochondria and synapses (in CNS), as a main component of their membrane cells. DHA's concentration is highest in the brain, particularly in synapses, and in vertebrate retina, which is the light-sensitive part of the inner surface of the eyes and it is necessary for the normal functioning of the eyes. The neurons are using DHA for exchange neurotransmitters for transit signals to a target cell. In that case if there are not enough DHA, DPA (Docosapentaenoic  $\omega$ -6 fatty acid) is used instead for exchange neurotransmitters, however the DHA is considered the best for this function. For example, the replacement of 22:6n-3 with 22:5n-6 that occurs in n-3 dietary deficiency, results in poorer retinal response in non-human primates [31, 32] and extends to complex phenotypes such as cognitive performance and behavior associated with central nervous system function [33].

Getting enough DHA in the human body is vital for childhood growth in that it aids normal development of the brain, eyes, and the CNS (central nervous system), and is also important for adulthood for the same reasons.

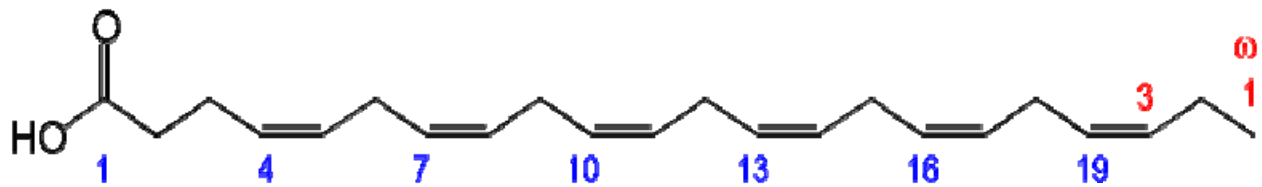


Figure 1.9. Docosahexaenoic acid

## 1.8. Lipid bilayer

Cell membranes consist of a phospholipid bilayer [34] (Figure 1.10), which is spontaneously arranged by phospholipids. As known, the phospholipids contain diglyceride (two fatty acids covalently bonded to a glycerol molecule through ester linkages), the phosphate group and headgroup. The most common headgroup in mammalian cells is the choline headgroup. Half of all mammalian cells have a choline head group. Phospholipids have an amphipatic character and they arrange the lipid bilayers corresponding to this amphipatic character. Particularly, the phospholipid's two hydrophobic tails are pointed to the core of lipid bilayer (the core or the center of

lipid bilayer does not have a water) and hydrophilic phosphate heads are pointed to the water on both sides of membrane.

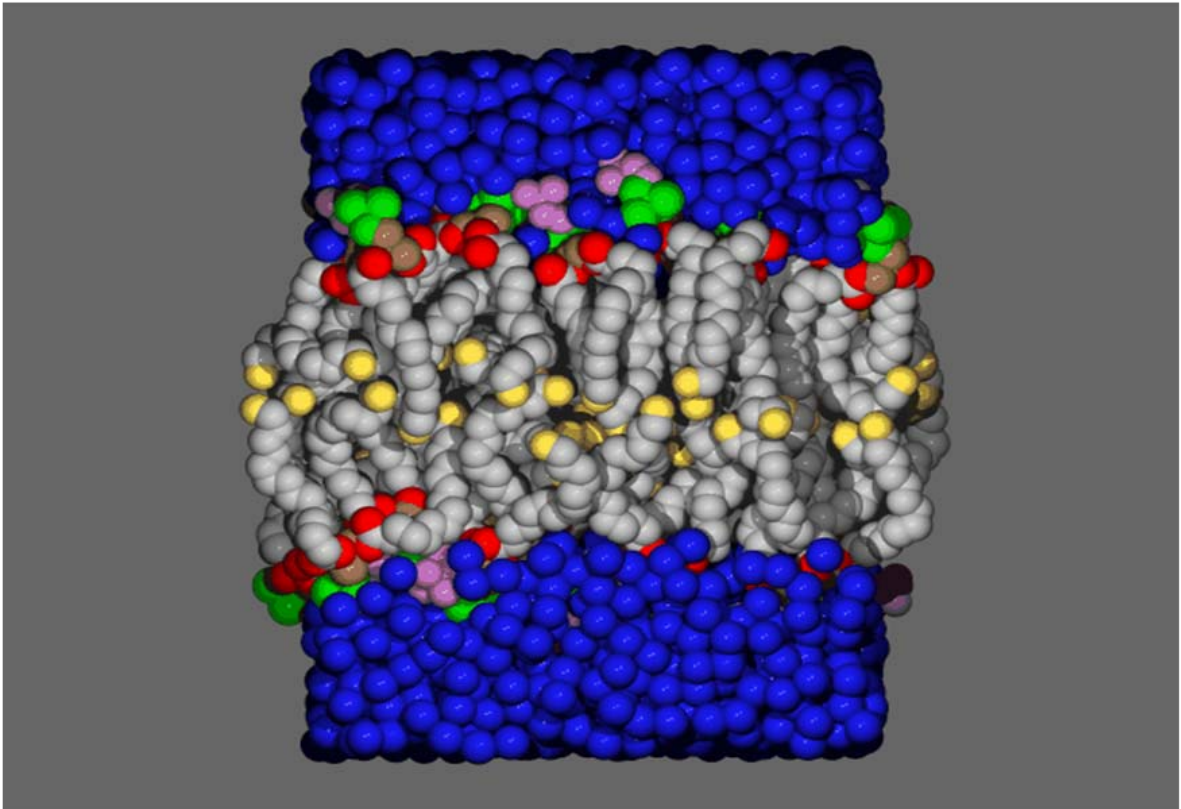


Figure 1.10: Phospholipid bilayer

The lipid bilayer in typical mammalian cells is a few nanometers thick, however, in spite of this the lipid bilayer has several different chemical regions. They are: hydrophobic core, partially hydrated intermediate region and fully hydrated hydrophilic region [35].

In spite of difficulties caused by the thickness and fragility, advanced experimental techniques, nuclear magnetic resonance [36], x-ray reflectometry [37], electron spin resonance [38], neutron scattering [39], allow to study the lipid bilayers and their regions.

## References

- [1] B. Alberts, A. Johnson, J. Lewis, M. Raff, K. Roberts, and P. Walter, *Molecular Biology of the Cell* (4th ed.). New York: Garland Science, 2002.
- [2] L.F. Kolakowski Jr, *Receptors Channels*, 2:1-7, 1994.
- [3] U. Gether, *Endocrine Reviews*, 21:90-113, 2000.
- [4] T. K. Attwood, and J. B. Findlay, *Protein Eng* 7: 195–203, 1994.
- [5] S. M. Foord, T. I. Bonner, R. R. Neubig, E. M. Rosser, J. P. Pin, A. P. Davenport, M. Spedding, and A. J. Harmar, *Pharmacol Rev* 57: 279–88, 2005.
- [6] K. Palczewski, T. Kumasaka, T. Hori, C. A. Behnke, H. Motoshima, B. A. Fox, I. Le Trong, D. C. Teller, T. Okada, R. E. Stenkamp, M. Yamamoto, and M. Miyano, *Science* 289:739-745, 2000.
- [7] T. Yoshizawa and G. Wald, *Nature* 197:1279-1286, 1963.
- [8] G.-F. Jang, V. Kuksa, S. Filipek, F. Bartl, E. Ritter, M. H. Gelb, K. P. Hofmann, and K. Palczewski, *J. Biol. Chem.* 276:26148-26153, 2001.
- [9] D. Pan and R.A. Mathies, *Biochemistry* 40:7929-7936, 2001.
- [10] D. S. Kliger and J. W. Lewis, *Israel J. Chem.* 35:289-307, 1995.

- [11] H. Kandori, Y. Yamazaki, Y. Shichida, J. Raap, J. Lugtenburg, M. Belenky, and J. Herzfeld, *Proc. Natl. Acad. Sci. USA* 98:1571-1576, 2001.
- [12] D. C. Teller, T. Okada, C. A. Behnke, K. Palczewski, and R. E. Stenkamp, *Biochemistry* 40:7761-7772, 2001.
- [13] D. Oesterhelt and W. Stoechenius, *Nat. New Biol.* 233:149-152, 1971.
- [14] S. Hayashi, E. Tajkhorshid, and K. Schulten, *Biophys. J.* 85:1440-1449, 2003.
- [15] R. A. Mathies, C. H. Brito Cruz, W. T. Pollard, and C. V. Shank, *Science* 240:777-779, 1988.
- [16] F. Gai, K. C. Hasson, J. Cooper McDonald, and P. A. Anfinrud, *Science* 279:1886-1891, 1998.
- [17] S. Ruhman, B. Hou, N. Friedman, M. Ottolenghi, and M. Sheves, *J. Am. Chem. Soc.* 124:8854-8858, 2002.
- [18] J. Saam, E. Tajkhorshid, S. Hayashi, and K. Schulten, *Biophys. J.* 83:3097-3112, 2002.
- [19] B. Isin, K. Schulten, E. Tajkhorshid, and I. Bahar, *Biophys. J.* 95:789-803, 2008.
- [20] A. H. Milam, Z. Y. Li, and R. N. Fariss, *Prog. Retin. Eye Res.* 17:175-205, 1998.
- [21] G. J. Farrar, P. F. Kenna, and P. Humphries, *The EMBO J.* 21:857-864, 2002.

- [22] H. F. Mendes, J. van der Spuy, J. P. Chapple, and M. E. Cheetham, *TRENDS in Mol. Medicine* 11:177-185, 2005.
- [23] L. Stryer, *Biochemistry* (4<sup>th</sup> edition), W.H. Freeman & Company, p. 328, 1995.
- [24] N. A. Campbell, B. Williamson, R. J. Heyden, *Biology: Exploring Life*, Boston, Massachusetts: Pearson Prentice Hall, 2006.
- [25] M. E. Chevreul. *Recherches chimiques sur les corps gras d'origine animale*. Paris, F. G. Levrault, 1823, p. 484.
- [26] J. Baruch. *Ber*, 27:172, 1894.
- [27] F. G. Edmed. *J. Chem. Soc.*, 73:627, 1898.
- [28] IUPAC. Compendium of Chemical Terminology, 2nd ed. (the "Gold Book"). Compiled by A. D. McNaught and A. Wilkinson. Blackwell Scientific Publications, Oxford (1997).
- [29] A. H. Lichtenstein. *Circulation*. 95:2588, 1997.
- [30] M. Singh, *Indian J. Pediatrics*, 72:239-242, 2005.
- [31] M. Neuringer, W. E. Connor, D. S. Lin, L. Barstad, and S. Luck, *Proc. Natl. Acad. Sci. USA*, 83:4021-4025, 1986.
- [32] G-Y. Diau, E. R. Loew, V. Wijendran, E. Sarkadi-Nagy, P. W. Nathanielsz, and J.

T. Brenna, *Invest Ophthalmol Vis Sci*, 2003. 44:4559-66, 2003.

[33] J-M. Bourre, M. Francois, A. Youyou, O. Dumont, M. Piciotti, G. Pascal, and G. Durand, *J. Nutr.* 119:1880-1892, 1989.

[34] S. E. Feller, K. Gawrisch, and T. B. Woolf, *J. Am. Chem. Soc.* 125: 4434-35, 2003.

[35] J. F. Nagle, S. Tristram-Nagle, *Biochim. Biophys. Acta* 1469:159–95, 2000.

[36] A. Grélard, C. Loudet, A. Diller, and E. J. Dufourc, *Methods Mol. Biol.* 654:341-59, 2010.

[37] B. A. Lewis, D. M. Engelman, *J. Mol. Biol.* 166 : 211–217, 1983.

[38] M. Ge and J. H. Freed, *Biophys. J.* 65:2106-2123, 1993.

[39] G. Zaccai, J. K. Blasie, B. P. Schoenborn, *Proc. Natl. Acad. Sci. U.S.A.* 72 : 376–380, 1975.

## Chapter 2

# Interaction between transmembrane proteins and phospholipids

### 2.1. Introduction

As discussed in Chapter 1, G-protein-coupled receptor (GPCR) rhodopsin, found in an environment rich in polyunsaturated fatty acids (PUFAs) and cholesterol, plays a crucial role in biological signaling processes. On the other hand, PUFAs with two or more double bonds found in higher terrestrial plants and mammals are composed predominantly of a series of non-conjugated double bonds in the *Z* (*cis*) and methylene-interrupted configuration, referred as “homoallylic”. The occurrence of homoallylic double bonds is generally ascribed to the reduction in melting point observed in the series 18:0, 18:1, 18:2, and 18:3 (18 and 0, 1, 2, 3 correspond to the numbers of carbon and double bonds, respectively). In animals, highly unsaturated fatty acids (HUFAs) are found most abundantly in the electrically excitable cells of the nervous system. The most common homoallylic HUFA in mammalian tissue is the hexaene docosahexaenoic acid (DHA) (22:6n-3), representing more than 10-35% of membrane fatty acyl groups in neuronal membranes. The disks of the retinal rod outer segments where rhodopsin resides is among the most unsaturated membranes,

consisting of phosphatidylcholine (PC) with 25% of fatty acids as the 22:6n-3, as well as long-chain unsaturated molecules with chain lengths up to C36.

However, not only rhodopsin and lipids themselves are of interest, but also their interactions, specifically those containing rhodopsin and highly polyunsaturated fatty acids [1-4]. The point is that the unique properties of polyunsaturated lipids suggest several mechanisms by which these lipids might interact with rhodopsin and influence its function in the retinal membrane. Many experimental works demonstrated that the presence of PUFAs in the membrane bilayer leads to dramatic changes in the activity of rhodopsin [5]. In particular, the presence of PUFAs in the membrane bilayer leads a significant lowering of cholesterol solubility [6-8]. It should be noted, that rhodopsin is sensitive to the membrane lipid composition, consequently, the influence of the different representatives of PUFA on the biological functioning of rhodopsin differs from each other. In particular, the substitution of 22:6n-3 with 22:5n-6 leads to reduced GPCR efficiency of rhodopsin, specifically rhodopsin-transducin coupling and phosphodiesterase activity [9]. Mechanistic explanations for these effects have focused overwhelmingly on the behavior of 22:6n-3-containing phospholipids interacting with one another in bulk membranes [10]. Measures of acyl chain intermolecular interaction in terms of melting, fluidity, and order parameters can be shown to differ dramatically between HUFA and saturated fatty acids, and even between 22:6n-3 and 22:5n-6. Most

models of 22:6n-3 action in biological systems have focused on bulk membrane properties [4], particularly partitioning away from lipid rafts, namely membrane domains enriched in certain lipids, cholesterol and proteins [11]. Situations in which direct interaction between membrane lipids and proteins have been considered theoretically have focused primarily on the differences between highly unsaturated fatty acids such as 22:6n-3 and saturated molecules such as 16:0. Calculations have suggested that attractive sites differ for the two extremes in hydrocarbon saturation [1], but these differences do not convey any information as to why 22:6n-3 and 22:5n-6 might differ so dramatically in their function due to the difference in one double bond.

Another interesting study indicating the importance of one double bond is work by Eldho et al. [12], in which the significant differences between 22:6n-3 and 22:5n-6 were detected. In particular, studying 22:6n-3 and 22:5n-6 by NMR, X-ray diffraction and molecular dynamics simulations Eldho and co-workers [12] found the following: (i) DHA chain is more flexible at the methyl group area than DPA chain; (ii) the density near the lipid/water interface for DHA is higher than for DPA; (iii) DHA isomerizes with shorter correlation time than DPA.

Recently, Feller [4] show that the conformational energetic of the DHA acyl chain is a very important feature, which can be considered as a key for understanding the properties of this fatty acid. In particular, low torsional energy barriers found for

the rotatable bonds in the DHA chain are the explanations to the differences between polyunsaturated and saturated acyl chains.

Rod outer segment membranes have long been known to be composed of about equal parts protein and lipid [13], which necessarily indicates that there is relatively little bulk phospholipid, with much in direct molecular contact with protein. Although there is some recent focus on weakly specific DHA - rhodopsin interactions [14], specific interactions between proteins and homoallylic groups have not been considered to any great extent. In addition to 22:6n-3, the rod-outer-segment membrane phospholipid fatty acyl chains have about 10% very long-chain PUFA (VLCPUFA) with carbon atoms from C26-36 detected in the retina more than two decades ago [15, 16]. They are located predominantly at the sn-1 position of PC (sn-1 shows a position of carbon atom in glycerol backbone, where the fatty acid is covalently bonded to a glycerol molecule) replacing saturated molecules and thus typically paired with 22:6n-3. They have recently been associated with Stargardt disease and thus appear to be of crucial importance [17] but there is no clearly understood function.

We propose a novel conformation between the extended homoallylic motif of PUFA, specifically, 22:6n-3, and transmembrane  $\alpha$ -helices that may confer unique functional properties on proteins embedded in highly unsaturated membranes. We propose that the extended homoallylic double bond system may be arranged in

intimate contact with, and follows, the groove of, the  $\alpha$ -helix. A first issue in establishing the plausibility of this proposal is to establish that this arrangement is not sterically forbidden, and specifically whether the hydrogen-bond structure of the  $\alpha$ -helix may remain intact with the hydrocarbon chain positioned in the groove. By means of a structural model, energy minimization, and molecular dynamics, we explore whether the homoallylic motif of 22:6n-3 and the VLCPUFA 34:5n-3 as components of PC are sterically hindered from residing in the groove of an  $\alpha$ -helix, using  $\alpha$ -helix-2 of bovine rhodopsin as a model.

## 2.2. Methods

A PC, PC-22:6-34:5, with 22:6n-3 in the sn-2 position and 34:5n-3 in the sn-1 position, was built and generated with the ChemOffice 10.0 suite (Cambridge). Bovine rhodopsin (PDB: 1L9H) helix 2 served as a model transmembrane helix. The homoallylic sections of the hydrocarbon chains were initially arranged to follow the groove of the alpha-helix. Energy minimization and short molecular dynamics (MD) simulations were performed with the GROMACS simulations package [18] using the GROMOS96 force field [19]. The time step was 2 fs, the temperature was set to 310 K, and the pressure to 1 bar using a Berendsen thermostat and barostat, [20] with coupling times of 0.1 and 1 ps, respectively. Although the GROMOS96 force field was developed with a twin-range cut-off of 0.8/1.4 nm, we used the Particle-Mesh

Ewald method [21, 22] for the calculation of long-range electrostatic interactions; 0.9 nm was used for the van der Waals cut-off. The steepest descent algorithm with a tolerance of  $200 \text{ kJ mol}^{-1} \text{ nm}^{-1}$  and maximum step size 0.01 nm was used for energy minimization. In order to keep the helix and lipid close to each other, distance restraints of  $10 \text{ \AA}$  between the atoms of the helix groove and the lipid were applied during the MD simulations; however, the distances between the specified pairs of atoms never approached this restriction limit during the short time MD simulations. Therefore, MD simulations were used effectively without restraints.

The initial positions were judged feasible because the energy minimization converged without disrupting the helix-lipid complex. The energy-minimized structures were examined for the conformation between atoms of the lipid hydrocarbon chains, including the lengthy homoallylic structure. Molecular dynamics simulations were run to establish whether the energy minimized system was stable over 10 ps and then inspected for atomic distances between helix and lipid.

### **2.3. Results**

The interactions of the second helix of rhodopsin with DHA, DPAn-6 and Glycerophosphocholines, which are the most important components of lipid bilayer, containing DHA and DPAn-6 were studied. The approach is based on two

hypotheses. The first hypothesis is that DHA can have the unstrained configuration, which allows wrapping around the groove of  $\alpha$ -helices of transmembrane proteins. In other words, DHA can fit into the groove. Second hypothesis is that DPAn-6 is unable to interact with  $\alpha$ -helices of transmembrane protein as close as DHA since saturated hydrocarbon regions do not fit into the groove as loosely as DHA. Based on these hypotheses we tried to find out the influence of steric effects for DHA and DPAn-6 wrapped around the main groove of  $\alpha$ -helices. In other words, whether the homoallylic hexaene moiety of DHA and DPAn-6 is sterically hindered, and define the difference of favorability of steric factors between the DHA and DPAn-6.

First, we tried to answer the following question: Can either DHA or DPAn-6 obtain wrapped form around the  $\alpha$ -helix of transmembrane bovine rhodopsin? We have proposed conformation for DHA and DPAn-6 shown in Figure 2.1.

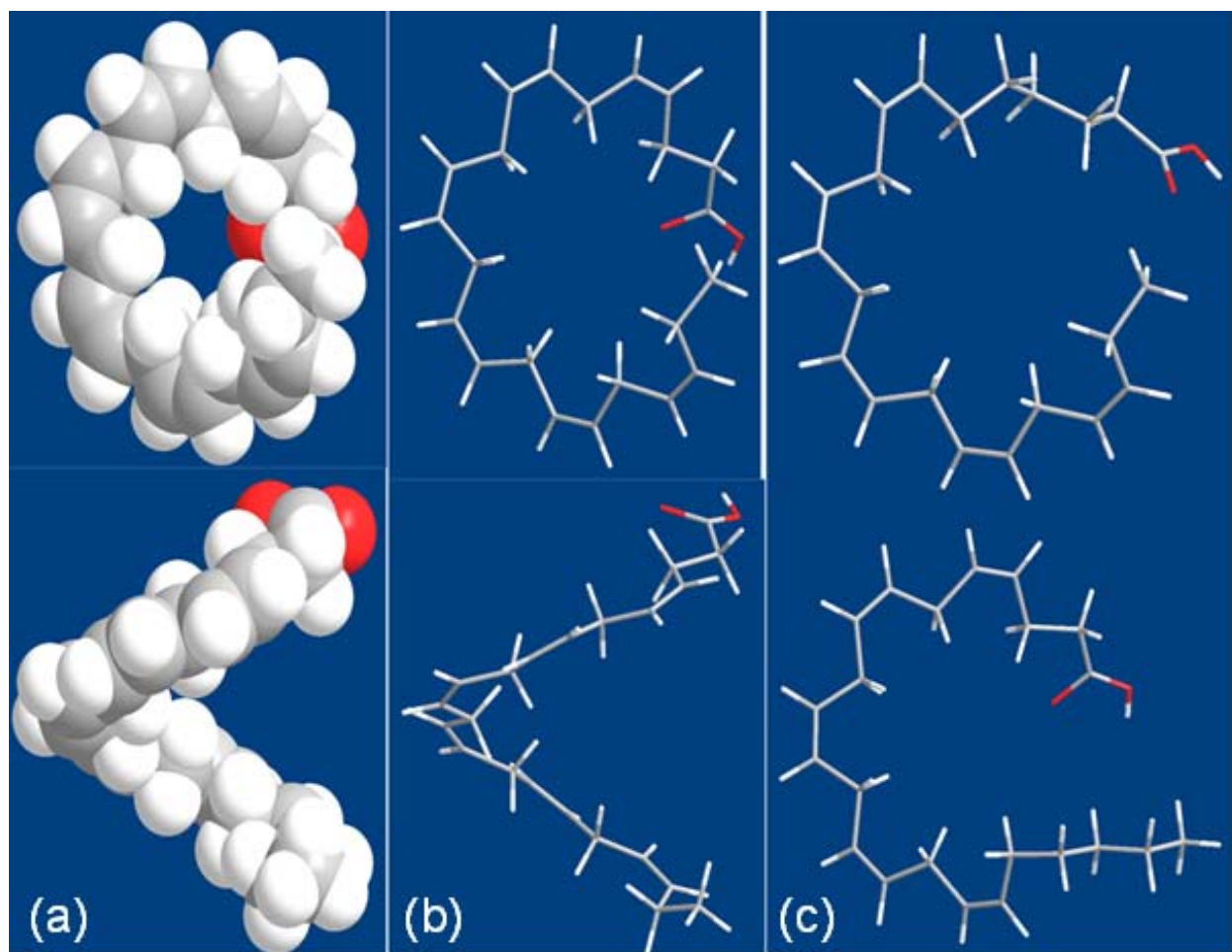


Figure 2.1: 22:6n-3 [in space-filling (a) and stick (b) models], 22:5n-3 [upper in panel (c)] and 22:5n-6 [lower in panel (c)] can assume a helical path that can follow the path of a transmembrane  $\alpha$ -helix. The atoms in red correspond to oxygens.

The *cis* double bonds can be arranged with the ethylenic hydrogens directed toward the center of alpha-helix groove and the doubly allylic  $-\text{CH}_2-$  directed out of center of alpha-helix groove. Considering hard sphere atoms, 22:6n-3 with six double bonds arranged in a plane would complete a  $360^\circ$  ring with the terminal methyl group occupying the same space as the carboxyl group, and thus sterically impossible without an incline. The n-6 analogue with only five double bonds does not have this overlap unless the saturated terminal region is directed to the carboxyl. The *cis* double bonds lock the  $\text{sp}^2$  C to a  $120^\circ$  planar configuration that occupies less space than  $\text{sp}^3$ . The homoallylic conformation provides a  $109^\circ$  ( $\text{sp}^3$  bond angle) bend in between *cis* double bonds which in turn limits the conformations possible in the chain as a whole. The helical conformation of 22:6n-3 is similar to the groove shape of protein  $\alpha$ -helices, including, of course, transmembrane  $\alpha$ -helices.

### 2.3.1. DHA-helix vs DPAn-6-helix

We performed the simulations to find out how DHA and DPAn-6 behave during the dynamics and if there are different steric effects among them during the dynamics.

First, we built the DHA and DPAn-6 fatty acids models, then the fatty acids were docked to the second  $\alpha$ -helix of bovine rhodopsin, and MD simulations were

carried out for the second helix of rhodopsin – DHA, and the second helix of rhodopsin – DPAn-6 systems. The final structures of fatty acids obtained from MD simulations were inspected for analysis of steric effects. For initial structures of DHA and DPAn-6 we used the conformation shown in Figure 2.2.

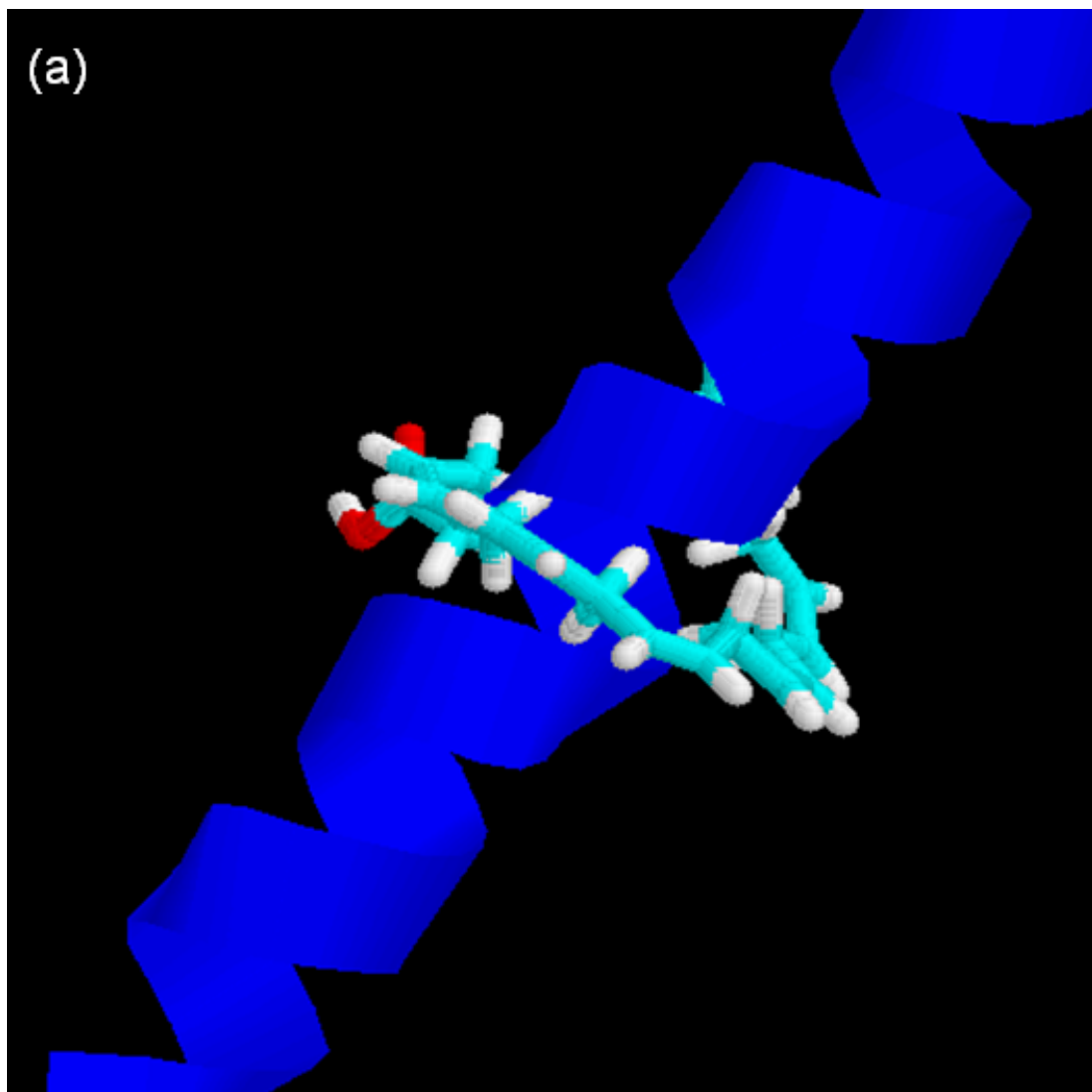


Figure 2.2 (Continued)

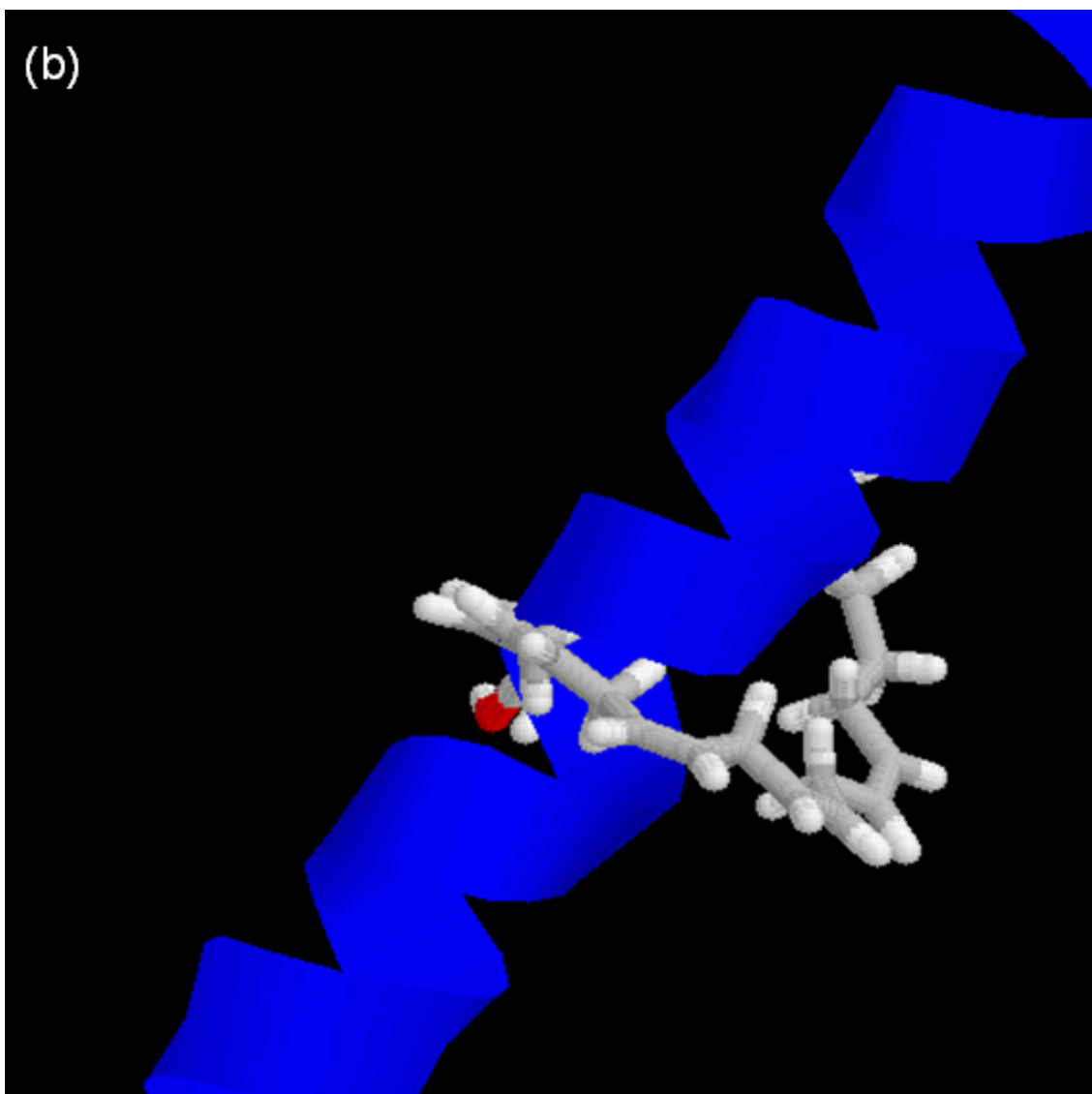


Figure 2.2: Proposed conformations of initial structure for DHA (a) and DPAn-6 (b) along with  $\alpha$ -helix.

We examined the structures of DHA and DPAn-6 after minimization, and after 10 ps restricted MD simulations for two different positions of the fatty acids: (i) fatty acids are in the middle of  $\alpha$ -helix (Figure 2.3); (ii) fatty acids are on the top of the  $\alpha$ -helix (Figure 2.4). In particular, we carried out the calculations for the following systems: (A) DHA wrapped around the  $\alpha$ -helix in the middle [Figure 2.3 (a,b,c)]; (B) DPAn-6 wrapped around the  $\alpha$ -helix in the middle [Figure 2.3 (d,e,f)]; (C) DHA wrapped around the  $\alpha$ -helix on the top [Figure 2.4 (a,b,c)]; (D) DPAn-6 wrapped around the  $\alpha$ -helix on the top [Figure 2.4 (d,e,f)]. For each A, B, C, and D we performed several MD simulations with different initial positions.

It should be noted, that starting from the same initial positions the final structures of DHA and DPAn-6 fatty acids obtained after minimization and restricted MD simulations have some similarities and differences (Figure 2.5). The similarities are the following: the homoallylic double bond systems of both DHA and DPAn-6 follow the groove and for both DHA and DPAn-6 doubly allylic hydrogens are directed into the helix and the ethylenic hydrogens are directed out of  $\alpha$ -helix. The difference is that the saturated region of DPAn-6 from methyl end breaks the helical homoallylic double bond system symmetry and this region moves out of  $\alpha$ -helix groove, while the saturated region of DHA from methyl end is shorter and this part follows the groove almost as well as the homoallylic double bond system.

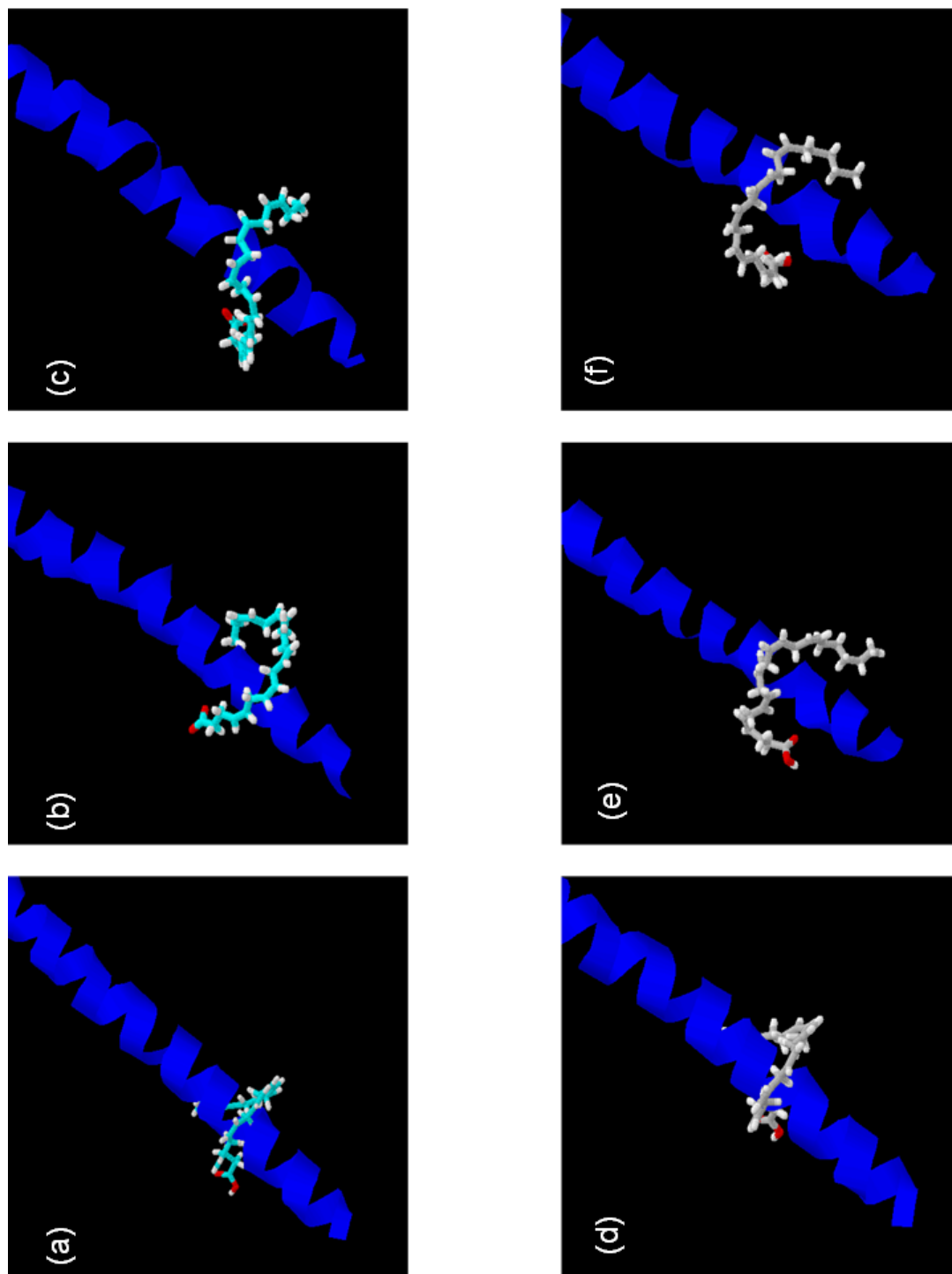


Figure 2.3. Initial (a,d), after minimization (b,e) and restricted molecular dynamics (c,f) positions of DHA and DPAn-6, respectively, wrapped in the middle of helix. The carbon chains of DHA and DPAn-6 are illustrated in cyan and grey color, respectively.

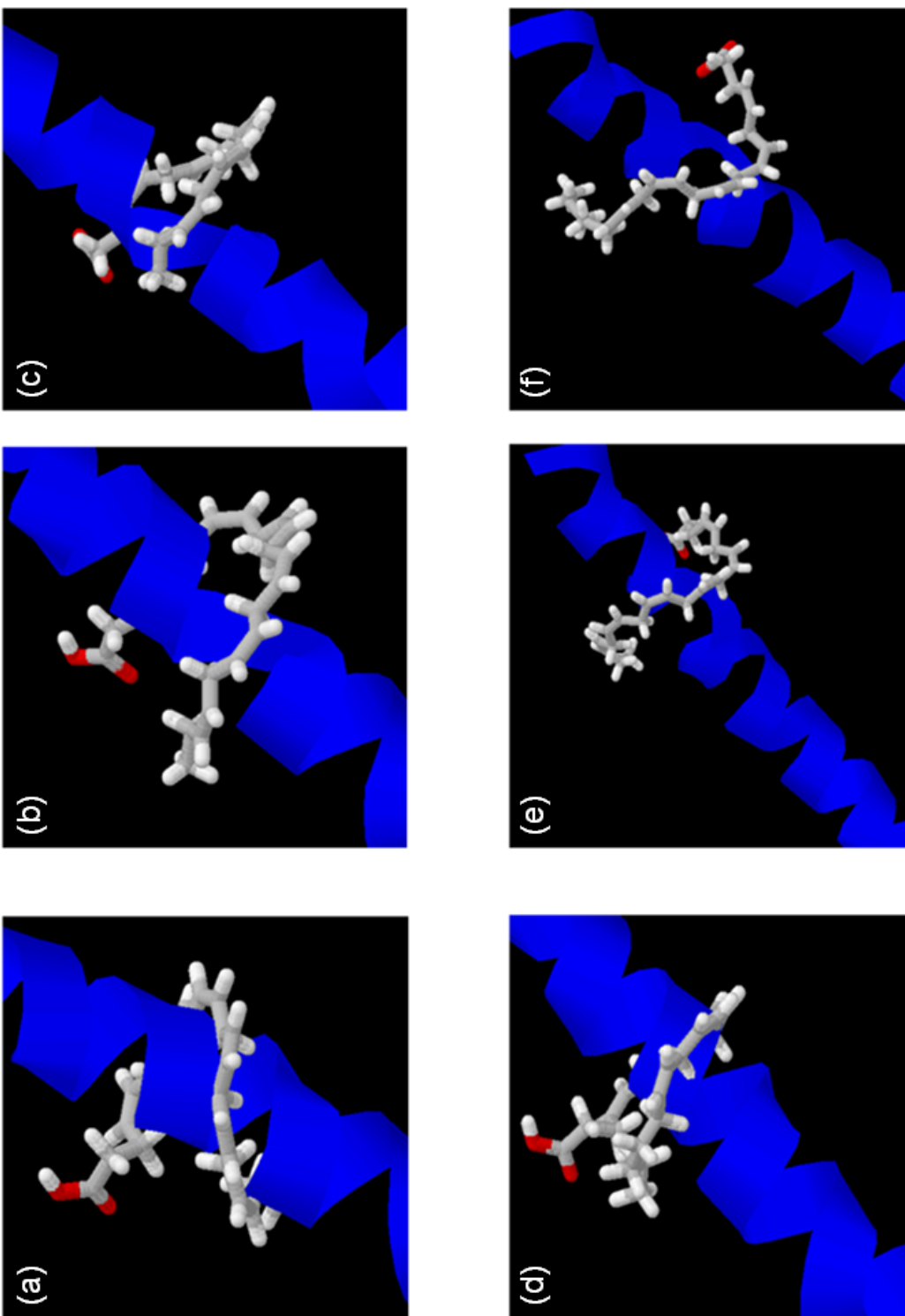


Figure 2.4. Initial (a,d), after minimization (b,e) and restricted molecular dynamics (c,f) positions of DHA and DPAn-6, respectively, wrapped on the top of helix. The carbon chains of DHA and DPAn-6 are illustrated in grey color.

Based on these results, we can conclude that extra double bond of DHA helps to interact more close to  $\alpha$ -helix groove than does DPAn-6.

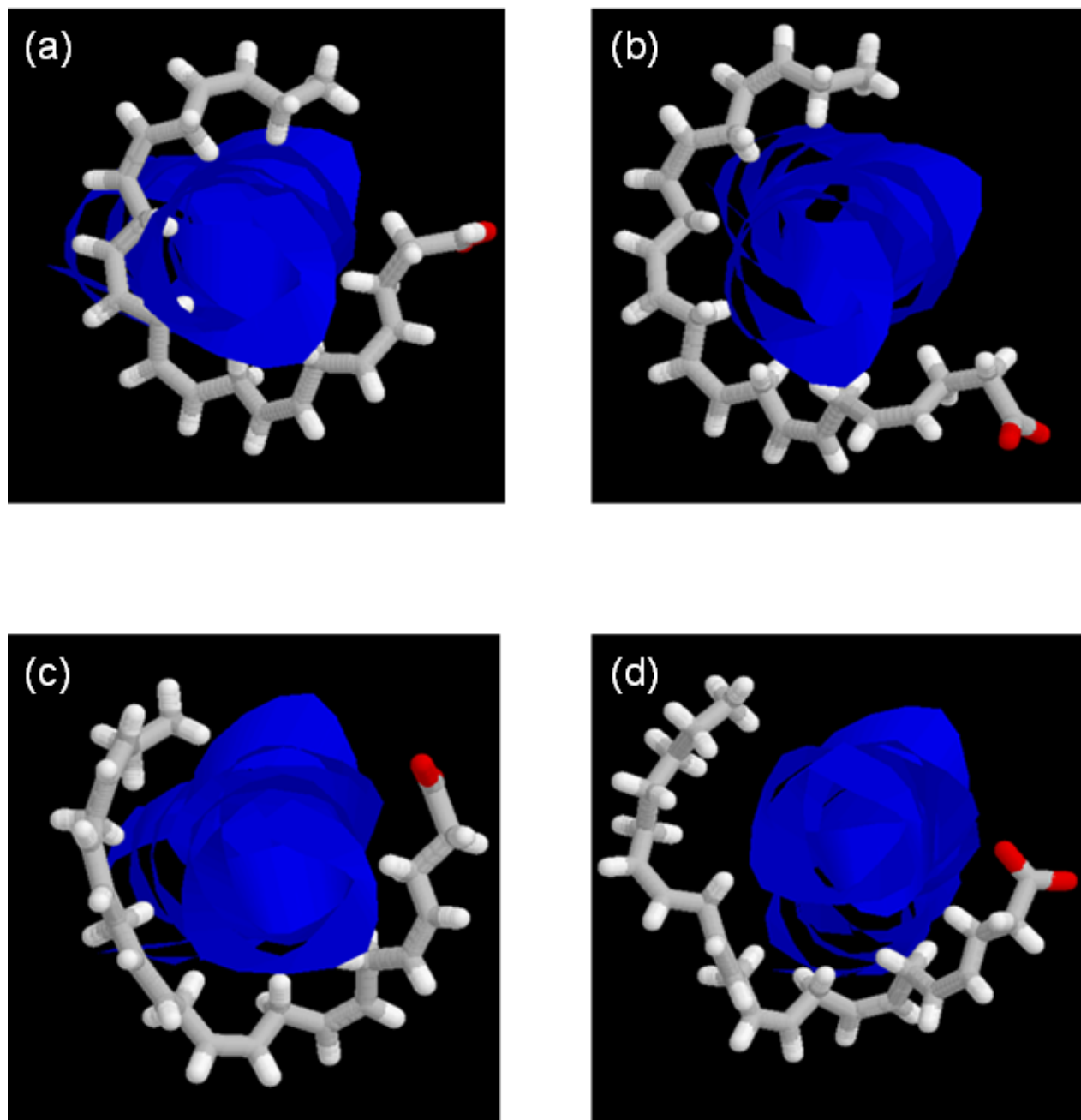


Figure 2.5. DHA and DPAn-6 after minimization (a,c) and restricted molecular dynamics (b,d), respectively.

### **2.3.2. Highly unsaturated homoallylic hydrocarbons may form a secondary helix in the groove of transmembrane protein $\alpha$ -helices**

For further examination of our hypotheses we performed the calculations on two different systems: (i) PC-22:6-34:5 with 22:6n-3 in sn-2 position and 34:5n-3 in sn-1 position along with second  $\alpha$ -helix of bovine rhodopsin; (ii) PC-22:5-34:5 with 22:5n-6 in sn-2 position and 34:5n-3 in sn-1 position along with second  $\alpha$ -helix of rhodopsin. In order to find out whether the saturated regions of 22:6n-3 of PC-22:6-34:5 and 22:5n-6 of PC-22:5-34:5 fit into the groove of  $\alpha$ -helix, and if so, how different are the steric effects of these regions, we first wrapped the lipids around the  $\alpha$ -helix. Figure 2.6 presents the initial arrangements for PC-22:6-34:5 (panel a) and PC-22:5-34:5 (panel b) shown in stick form docked with the  $\alpha$ -helix shown as a ribbon for clarity. The initial positions correspond to glycerophospholipids amphipatic character, where the hydrophilic head-choline is placed outer surfaces of cell membrane and hydrophobic tails are directed into center of phospholipids bilayer. The 22:6n-3 and 22:5n-6 hydrocarbon chains follow the helix groove closest to the water interface, while the saturated sections of 34:5n-3 in both lipids are shown tethering the homoallylic section to a groove three turns towards its center.

(a)

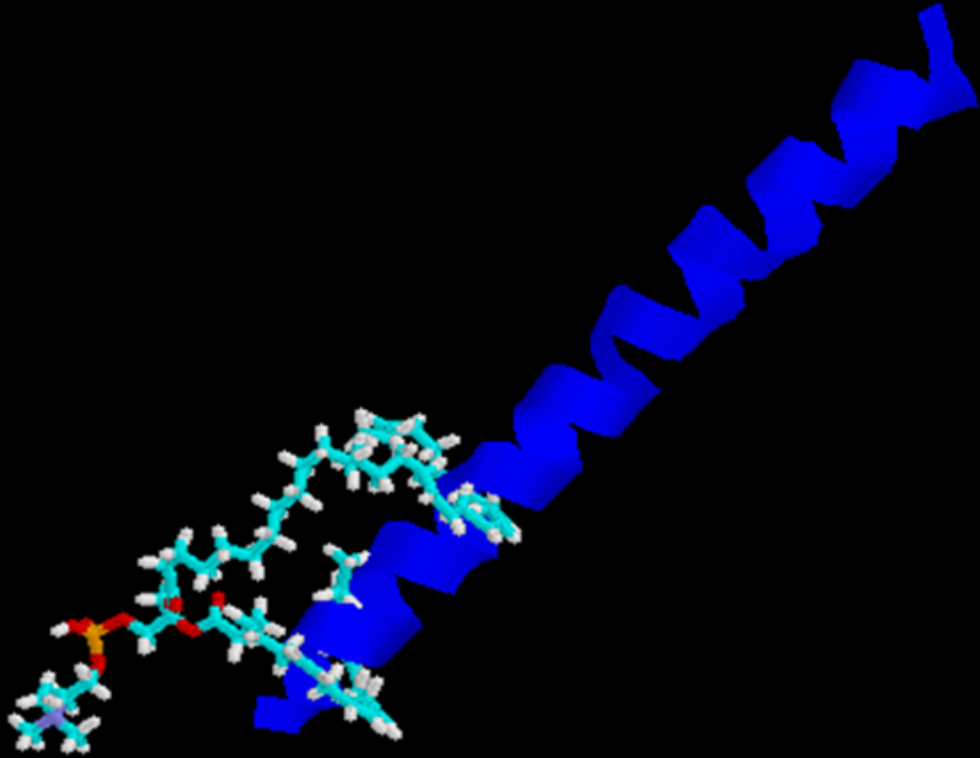


Figure 2.6 (Continued)

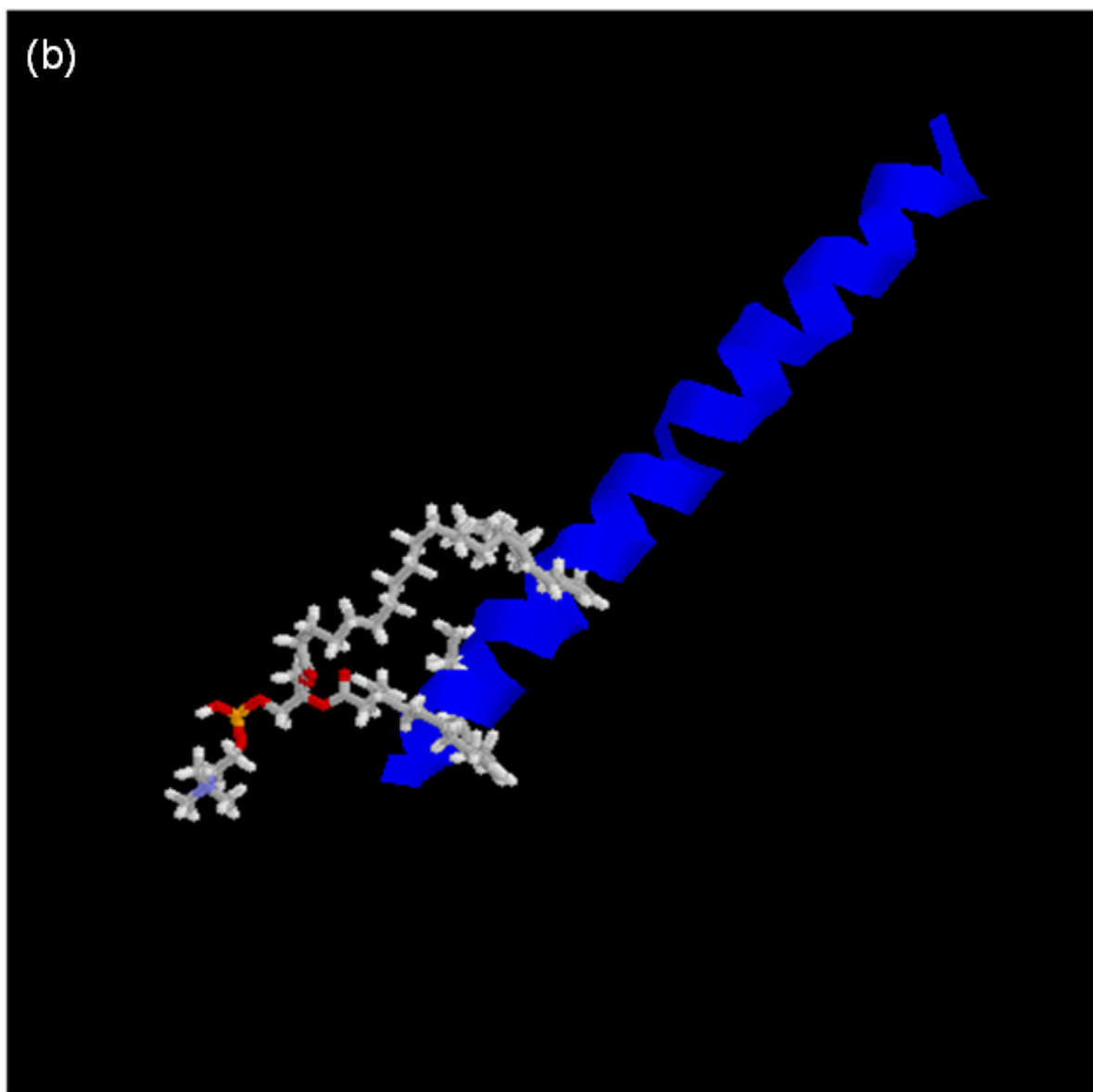


Figure 2.6: Initial structure of PC-22:6-34:5 (a) and PC-22:5-34:5 (b) docked at the end of helix 2 of bovine rhodopsin.

In order to find out quantitatively whether the saturated regions of the 22:6n-3 of PC-22:6-34:5 and 22:5n-6 of PC-22:5-34:5 fit into the groove, we did the following measurements:

(i) First, the lengths of the corresponding saturated regions were measured for both glycerophospholipids and have compared to each other. The length of the saturated region of 22:6n-3 of PC-22:6-34:5, shown in green color in Figure 2.7 (panel a), is 3.8 Å, while the length of the saturated region of 22:5n-6 of PC-22:5-34:5, shown in green color in Figure 2.7 (panel b), is 8.3 Å.

(ii) Second, the spaces occupied by the saturated region of 22:6n-3 of PC-22:6-34:5 (panel a in Figure 2.8) and 22:5n-6 of PC-22:5-34:5 (panel b in Figure 2.8) were measured. The saturated region of docosahexaenoic acid, 22:6n-3, has only one group of CH<sub>2</sub>, which takes a space of size 0.74Å; 0.74Å and 2.45Å, where 0.74Å is the diameter of hydrogen (shown in panel a) and 2.45Å is the distance between the hard sphere surfaces of hydrogens plus their diameters (shown in panel b). The saturated region of 22:5n-6 has four groups of CH<sub>2</sub> and, consequently, takes more space in the groove.

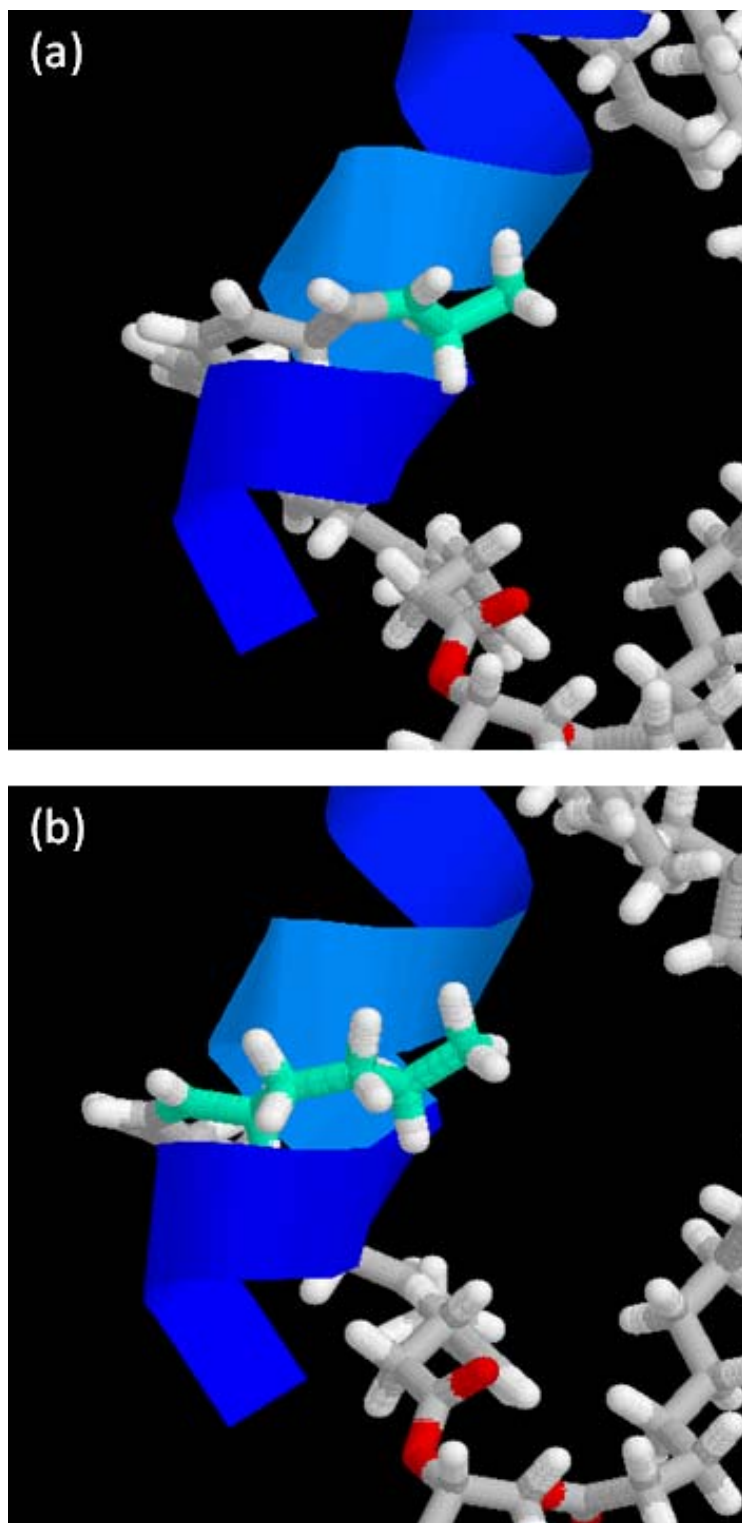


Figure 2.7 PC-22:6-34:5 (a) and PC-22:5-34:5 (b) and  $\alpha$ -helix.

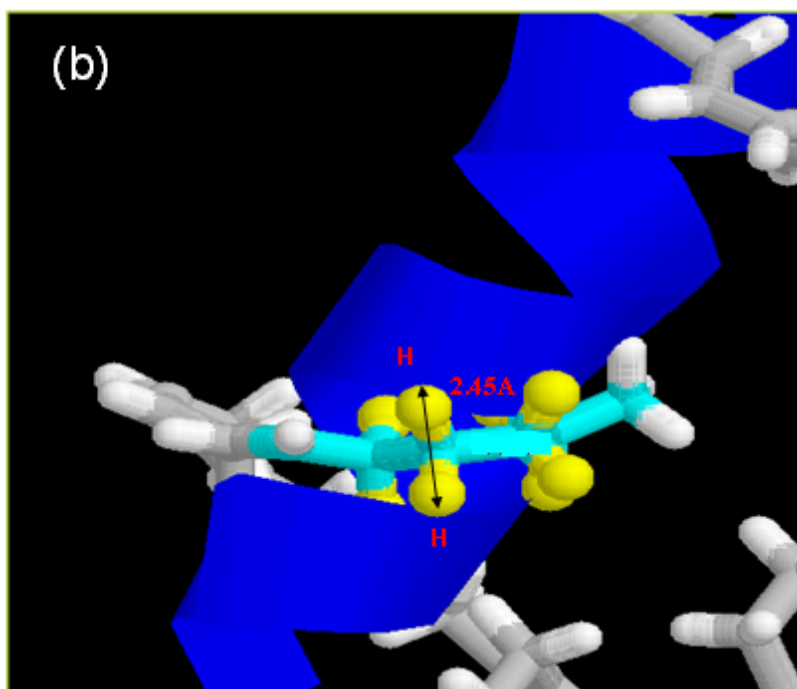
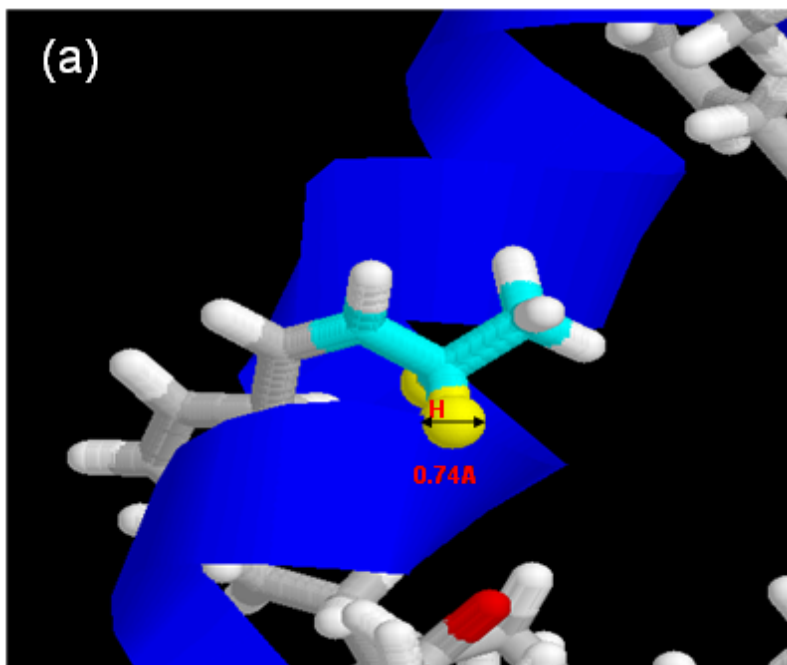


Figure 2.8. PC-22:6-34:5 and helix (a) and PC-22:5-34:5 and helix (b). The saturated regions of 22:6n-3 and 22:5n-6 are in cyan color, and hydrogen atoms are in yellow color.

(iii) Last, the size of the groove of  $\alpha$ -helix, where the saturated region of glycerophospholipid is located, was measured. More specifically, the smallest size of the closest part of alpha-helical groove to 2nd and 3rd carbons from methyl end, where the saturated region of 22:6n-3 of PC-22:6-34:5 is located, was measured (Figure 2.9).

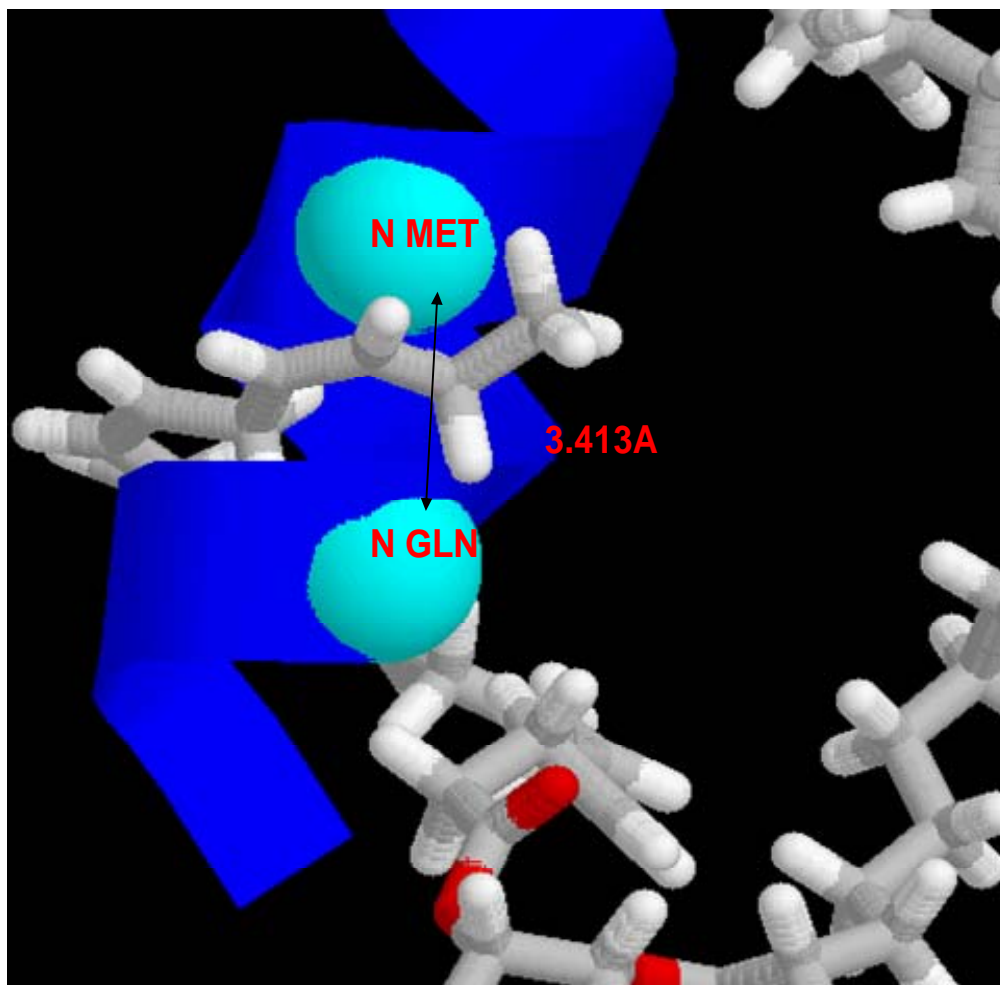


Figure 2.9: The distance between the surfaces of N MET and N GLN is 3.413Å. The cyan color atoms are N's of Methionine and Glutamine. They are shown in spacefill models.

We also measured the distance between the hard sphere surfaces of Hydrogens (which belong to 3rd carbon from methyl end) for both 22:6n-3 and 22:5n-6, and Nitrogens belong to Methionine and Glutamine. The distance between the hard sphere surfaces of Hydrogen of 22:6n-3 and Nitrogen of Methionine is 1.02Å (panel a in Figure 2.10) and the distance between the hard sphere surfaces of Hydrogen (the closest H to N) of 22:5n-6 and Nitrogen of Methionine is 0.17Å (panel b in Figure 2.10). The distance between the hard sphere surfaces of Hydrogen of 22:6n-3 and Nitrogen of Glutamine is 2.10Å (panel c in Figure 2.10) and the distance between the hard sphere surfaces of Hydrogen (the closest H to N) of 22:5n-6 and Nitrogen of Glutamine is 1.05Å (panel d in Figure 2.10).

Based on the measurements shown above, it was analyzed how well the saturated regions of 22:6n-3 of PC-22:6-34:5 and 22:5n-6 of PC-22:5-34:5 can fit into the groove at initial position. In particular, it was concluded that (i) both saturated regions can fit into the groove of  $\alpha$ -helix (ii) the saturated region of 22:6n-3 of PC-22:6-34:5 can fit more loosely into the groove than the saturated region of 22:5n-6 of PC-22:5-34:5; (iii) because of its flexible nature, bigger length and occupied space the saturated region of 22:5n-6 of PC-22:5-34:5 has more probability to move out and do not follow the groove than the saturated region of 22:6n-3 of PC-22:6-34:5 during minimization and MD simulations.

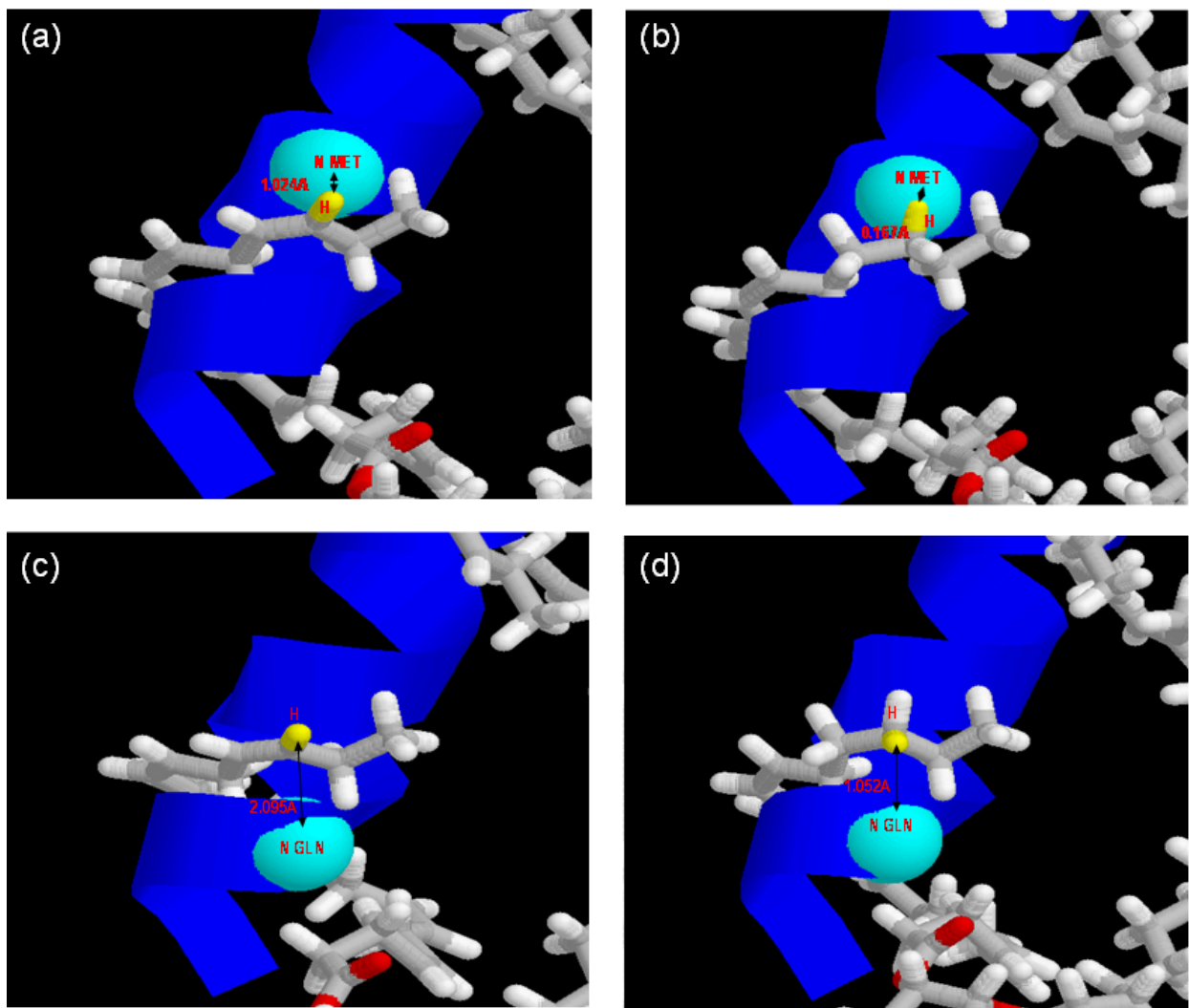


Figure 2.10: PC-22:6-34:5 and helix (a, c) and PC-22:5-34:5 and helix (b, d). Nitrogen atoms are in cyan color, Hydrogen atoms are in yellow color.

Since the saturated region of 22:6n-3 of PC-22:6-34:5 can loosely fit into the groove of  $\alpha$ -helix, the next step was the minimization of the system: PC-22:6-34:5 and second helix of bovine rhodopsin (see Figure 2.11). The analysis of the structure of the system after minimization shows that the homoallylic sections of 22:6 and 34:5( $\omega$ 3) in PC-22:6-34:5 are planar and they remain within the alpha-helix groove and follow it. For both 22:6 and 34:5( $\omega$ 3) sections, doubly allylic hydrogens are directed into the helix, while the ethylenic hydrogens are directed out of helix. The helix remains intact, indicating that the hydrocarbon chain is not sterically forbidden from occupying the space of an intact helix.

Representative spacing between an outwardly-directed ethylenic hydrogen and the protein helix is presented in Figure 2.12. The region from C16-C20 region of 22:6n-3 is zoomed to show the final two double bonds, and space-filling nitrogens of the helix. These atoms of closest approach form boundaries between (N Met) and (N Gln) atoms. The hard sphere distances are  $\sim 1.0 \text{ \AA}$  and  $\sim 2.1 \text{ \AA}$ , respectively. These distances indicate that the ethylenic hydrogen do not interact strongly with the  $\alpha$ -helix.

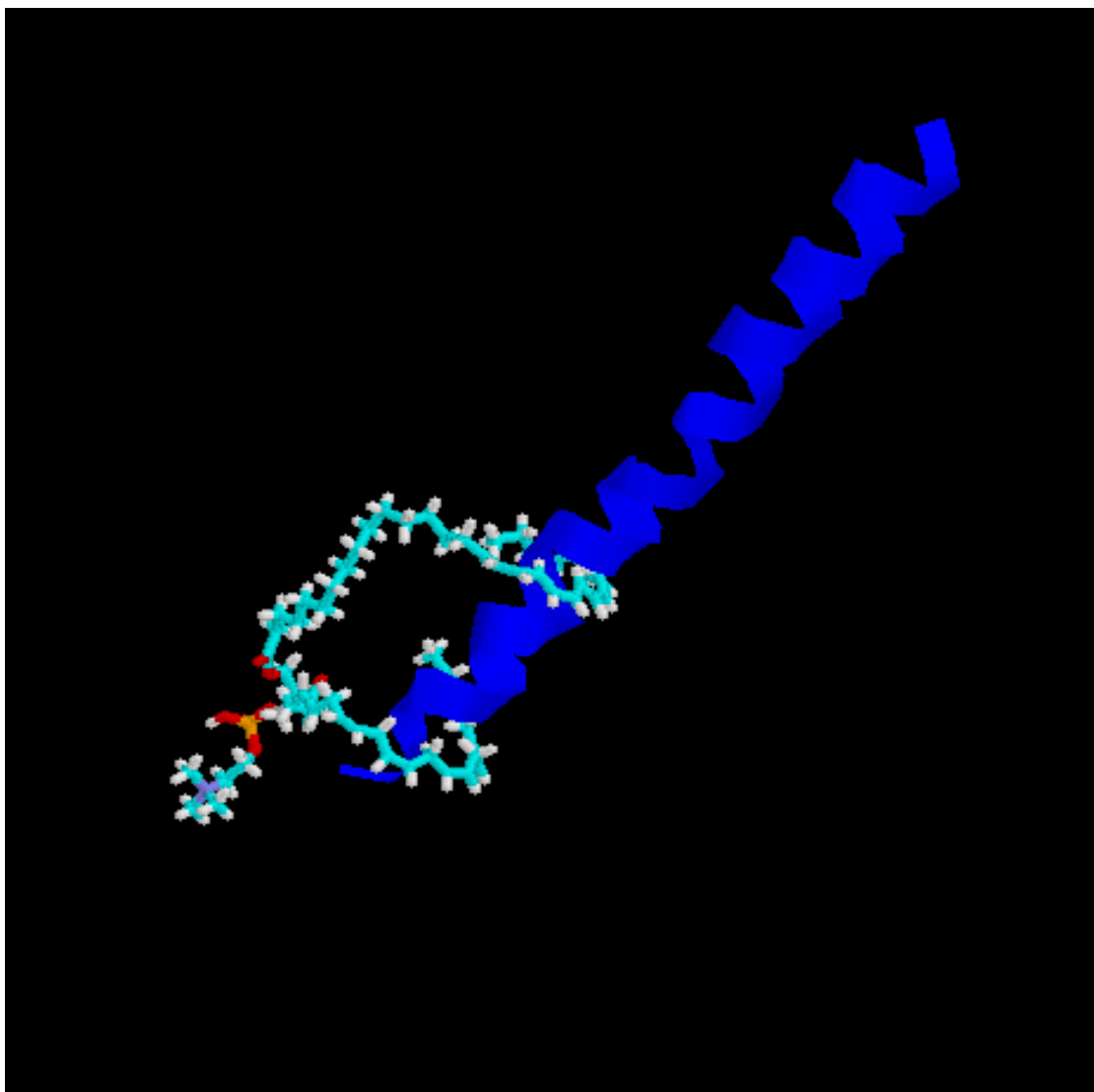


Figure 2.11: PC-22:6-34:5 and helix after minimization.

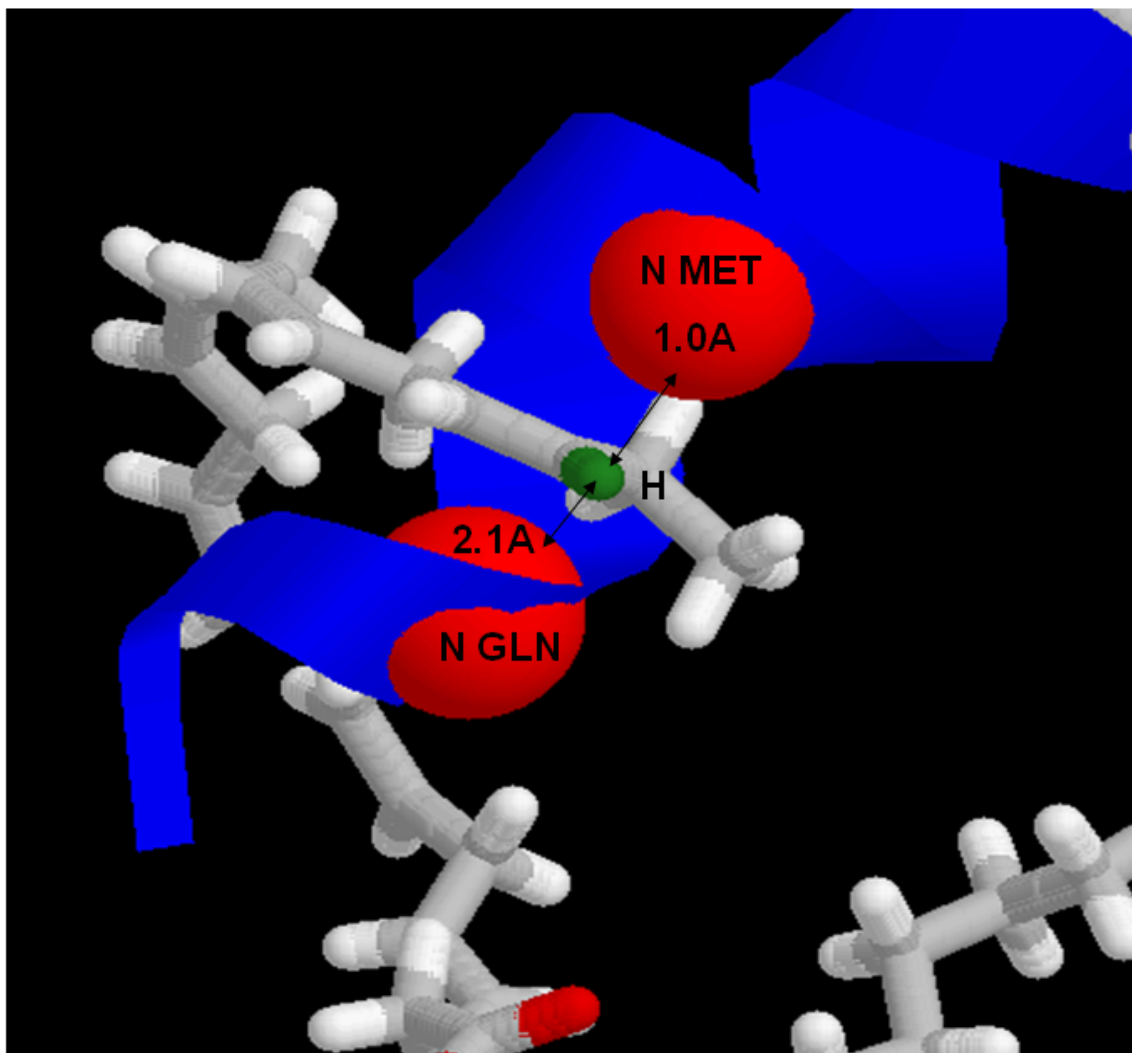


Figure 2.12: Expanded view of the ethylenic hydrogen (in green) on C20 of 22:6n-3, showing hard sphere distances between the closest helix atoms (in red), both nitrogens.

The doubly allylic hydrogens occupy more space in the groove and were examined more closely. Figure 2.13 shows the hydrogens of C18 in 22:6 in blue space-filling representation; the greatest distance from outer edges of these hydrogens

is 2.4 Å (not shown). As presented, the lower left side of the groove has a sequence of residues PRO-TRP-GLN while the complementary upper right has PHE-SER-MET-LEU, with the atoms closest to the hydrogens (shown in yellow). Table 2.1 presents the distances that define the hard sphere spacing of the groove, and all but three are greater than the 2.4 Å. The TRP-PHE distances are less than 2.4 Å, however, they are nearly parallel to the groove, where only allylic hydrogen with diameter ( $<0.7$  Å) is located, as is the SER-MET dimension on the upper left groove. Thus, these measurements show that the helix groove has ample space to contain doubly allylic hydrogens.

Two views of space-filling models are presented in Figure 2.14, with  $\alpha$ -helix colored red and lipid colored blue. The left view illustrates the tight docking between the lipid and the helix held together by the long saturated region of 34:5. The right view is from the opposite side and shows the positions of the terminal regions of the homoallylic chains. The center of the homoallylic region of the 34:5 chain is positioned tight to the helix and then the terminal methyl exits the groove. In contrast, the terminal methyl of the 22:6n-3 is seen to be within the groove and is partially buried by a Trp residue positioned on the helix turn closest to the water interface.

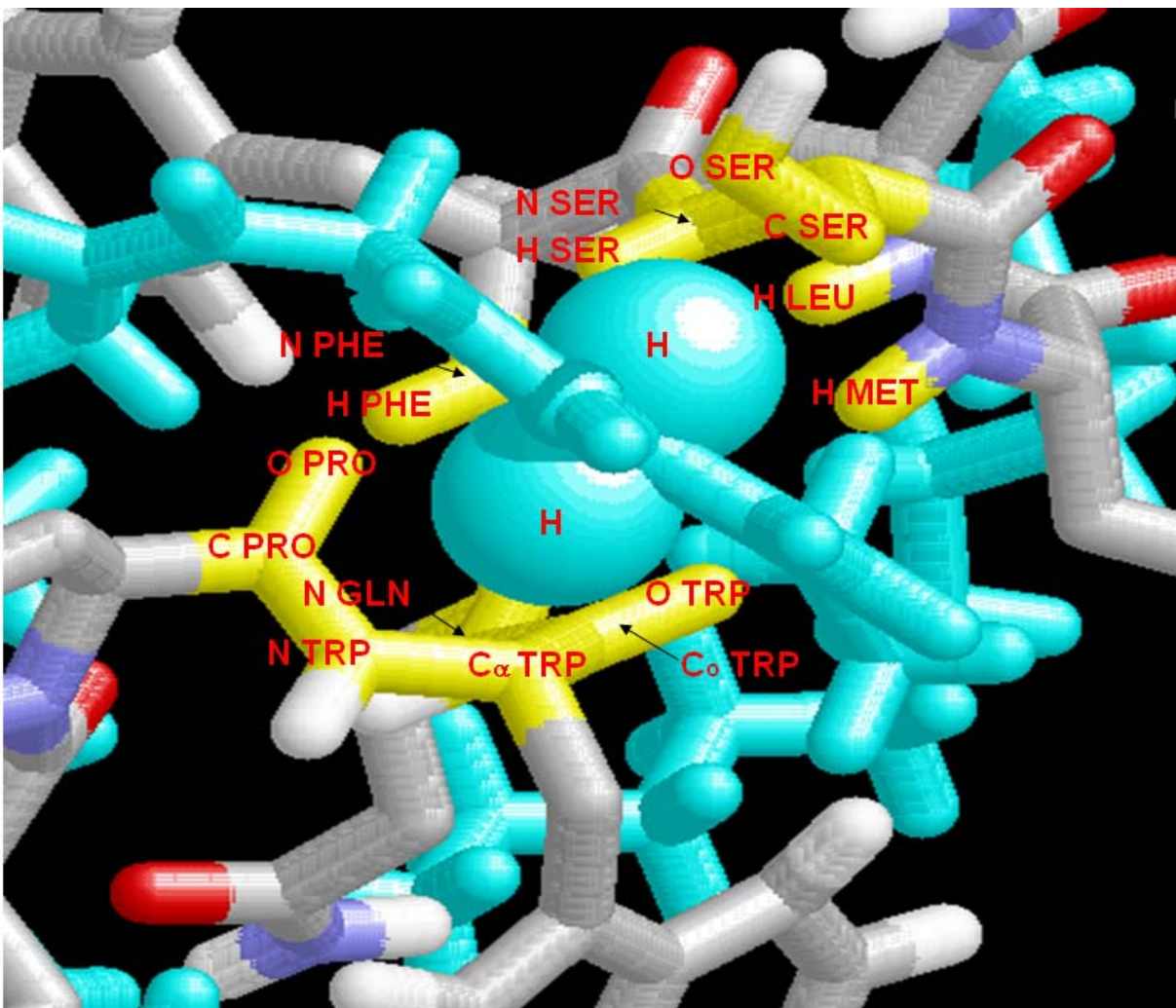


Figure 2.13: The first doubly allylic hydrogens from the methyl end are shown in a spacefill model. They belong to 22:6 of PC226345( $\omega$ 3) and are shown in blue color. The yellow-colored atoms belong to the second helix of rhodopsin.

Table 2.1: The distances between the atoms (in yellow) of the groove of  $\alpha$ -helix in the vicinity of C18, illustrated in Figure 2.12.

<u>Lower left side of groove</u>		<u>Upper right side groove</u>		Distance (Å)
Atom	Residue	Atom	Residue	
N	GLN	O	SER	5.3
N	TRP	C	SER	4.6
O	PRO	H	LEU	4.5
C <sub>α</sub>	TRP	O	SER	4.2
C <sub>α</sub>	TRP	C	SER	3.7
C <sub>o</sub>	TRP	C	SER	3.6
N	GLN	N	SER	3.4
C <sub>α</sub>	TRP	N	SER	2.9
C <sub>o</sub>	TRP	N	SER	2.8
O	TRP	H	PHE	2.3
C <sub>o</sub>	TRP	H	PHE	1.9
O	TRP	N	PHE	1.9
Closest residue atoms, upper left side				
H	SER	H	MET	2.2

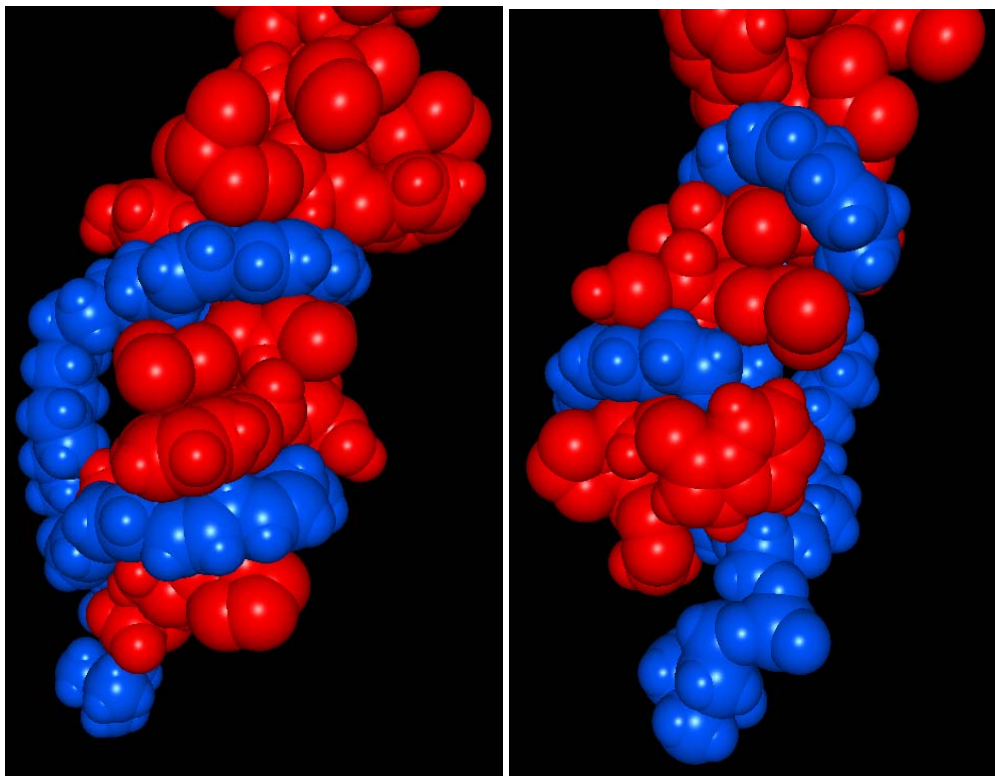


Figure 2.14: Space-filling energy-minimized model showing two opposing views of the homoallylic chains (blue) buried to the  $\alpha$ -helix (red). Left: View showing entry of the homoallylic chains from the glycerol backbone. Right: The 22:6 terminal methyl is buried within the groove of the  $\alpha$ -helix and covered by a TRP residue, while the terminal region of 34:5 extends out of the groove.

## 2.4. Discussion

The melting points of fatty acids are influenced by their contents of double bonds. There are several points of evidence to suggest that the melting points and interactions between hydrocarbon chains are not the sole biophysical property driving the appearance of HUFA, often in well conserved, high concentrations. (i) The relative difference in melting points are small for HUFA: the melting point for the C20 HUFA 20:4n-6 and 20:5n-3, differing in one double bond, are  $-50^{\circ}\text{C}$  and  $-54^{\circ}\text{C}$  respectively, while the melting point of 22:6n-3 is greater than either at  $-44^{\circ}\text{C}$ . Moreover, were the lowest melting point the driving force, 4,8,12,15,19-docosapentaenoic acid, with three ethylene-interrupted double bonds and a melting point of  $-78^{\circ}\text{C}$  [23], would be favored. All these values are well below environmental temperatures that support life of plants and poikilotherms (cold-blooded) at near atmospheric pressures. (ii) The brain [24] and liver [25] fatty acid composition of fish living in widely differing temperatures shows no discernable trends in HUFA composition with temperature despite clear trends in saturate and monounsaturate concentrations as well as membrane fluidity as measured by molecular probes .

The reduction in melting point occurs because homoallylic double bonds restrain the conformation of hydrocarbon chains such that they cannot closely interact in bulk or as components of membrane bilayers. They also increase the susceptibility of the hydrocarbon chain by appearance of doubly allylic hydrogen that

are especially prone to reaction with various forms of activated oxygen. Indeed, methyl branching is an alternative chemical modification to the normal hydrocarbon chain that also reduces intermolecular interactions, and melting points, and is widely used in microorganism membrane [26] and is inert to oxygen attack. Consistent with this observation is a very early report showing that an *E. coli* mutant with defective monounsaturated fatty acid synthesis and fatty acid degradation grew equally well on anteisopentadecanoate (12-methyl-tetradecanoate) or oleate (*9Z*-octadecenoate) [27]. Reliance on the homoallylic PUFA conformation, rather than methyl branching, may well involve unknown protein interactions.

Double helical protein-DHA phospholipids (PL) could explain how highly oxidizable DHA and other PUFA can exist in membranes such as the retinal outer segment disks and mitochondria where activated oxygen species due to light or metabolism are both at their highest. Double bonds are not solvent or O<sub>2</sub> accessible, and thus are stable indefinitely. The CNS is estimated to expend more than 20% of its considerable energy consumption in phospholipid metabolism, including acylation-reacylation of 22:6n-3 and 20:4n-6 [28], which enables replacement of PUFA damaged by oxidation. PUFA chains buried in a transmembrane helix would not be vulnerable to oxidative attack.

Stability of the double helical structure, once formed, may well be high. Rhodopsin, as other transmembrane proteins, has several transmembrane helices that

would pack densely and may prevent escape of the hydrocarbon chain. The terminal methyl of 22:6 buried by a TRP illustrates how a residue could stabilize the homoallylic chain within the groove, and may help explain why n-6 fatty acids are less favored if, for instance, molecular dynamics simulations or experiment showed the constraint of the n-3 configuration to be important to stability.

A possible function of this conformation is to anchor the transmembrane protein to the membrane. PL arranged as shown at top and bottom of all the helices, would in effect be interdigitated along the helix, packing tightly and anchoring the protein to the hydrated salt layer of the choline, or ethanolamine, headgroup. This role explains the VLCPUFA which can reach the second and, as shown, third helical turns in the interior of the membrane, further anchoring the protein to the membrane. This may be particularly important for proteins embedded in highly energy, electrically excitable membranes, and particularly for those proteins such as rhodopsin that change conformation during function.

## **2.5. Conclusions**

The main goal of this work was: (i) to find out the influence of steric effects for DHA wrapped around the main groove of second  $\alpha$ -helix of bovine rhodopsin, in other words, whether the homoallylic hexaene moiety of DHA is sterically hindered;

and (ii) to define the difference of favorability of steric factors between the DHA and DPAn-6.

Based on the initial structure, and conformations obtained after minimization and MD simulations for DHA and DPAn-6 along with second  $\alpha$ -helix of bovine rhodopsin, it was shown that (i) the doubly allylic hydrogens of DHA and DPAn-6 are directed into the helix and the ethylenic hydrogens are directed out of  $\alpha$ -helix; (ii) in verification of the first hypothesis stated in section 2.3, the homoallylic sections follow the  $\alpha$ -helical groove and there is more than one homoallylic section in one system, and they may have parallel conformations; (iii) Highly unsaturated homoallylic hydrocarbons may form a secondary helix in the  $\alpha$ -helices of transmembrane protein; (iv) in verification of the second hypothesis stated in section 2.3, the saturated region of DPAn-6 may move out and do not follow the groove of the  $\alpha$ -helix after minimization and MD simulations, while the homoallylic section stays inside the groove of  $\alpha$ -helix; (v) both the saturated region and homoallylic section of DHA follow and stay inside the groove of  $\alpha$ -helix.

In the end, it should be noted that the hypotheses on which this work was based have been verified for the studied systems with chosen initial conditions. For example, the calculations showed that a double hetero-helix is not sterically forbidden. Although there is, to our knowledge, no evidence that this structure exists in real

systems, or would be stable or confer unique biophysical properties, its plausibility and function can be speculated.

The calculations do not establish why 22:6n-3 is favored compared to 22:5n-6 in all neural tissue when n-3 fatty acids are available in an animal diet. Detailed molecular dynamics simulations are required to provide mechanistic insight as to whether thermal and possibly protein conformational changes in a fully assembled membrane would be more likely to retain unsaturated hydrocarbon regions. These will be appropriate once experiments to determine whether 22:6n-3 doubly allylic protons are in close proximity to the interior of biological transmembrane helices show that the hypothetical arrangement appears in nature.

## References

- [1] A. Grossfield, S. E. Feller, and M. C. Pitman, *Proc. Natl. Acad. Sci. USA*. 103:4888-4893, 2006.
- [2] A. Grossfield, M. C. Pitman, S. E. Feller, O. Soubias, and K. Gawrisch, *J. Mol. Biol.* 381:478-486, 2008.
- [3] O. Soubias, S. L. Niu, D. C. Mitchell, and K. Gawrisch, *J. Am. Chem. Soc.* 130:12465-1271, 2008.
- [4] S. E. Feller, *Chem. Phys. Lipids* 153:76-80, 2008.
- [5] S. E. Feller and K. Gawrisch, *Curr. Opin. Struct. Biol.* 15:416-422, 2005.
- [6] D. Hustauer, K. Arnold, and K. Gawrisch, *Biochemistry*, 37:17299-17308, 1998.
- [7] S. R. Wassall, M. R. Brzustowicz, S. R. Shaikh, V. Cherezov, M. Caffrey, and W. Stillwell, *Chem. Phys. Lipids* 132:79-88, 2004.
- [8] M. C. Pitman, F. Suits, A. D. MacKerell Jr, and S. E. Feller, *Biochemistry* 43:15318-15328, 2004.
- [9] S-L. Niu, D. C. Mitchell, S-Y. Lim, Z-M. Wen, H-Y. Kim, N. Salem, Jr., and B. J. Litman, *J. Biol. Chem.* 279:31098-31104, 2004.
- [10] K. Gawrisch and O. Soubias, *Chem. Phys. Lipids* 153:64-75, 2008.
- [11] S. R. Wassall and W. Stillwell, *Chem. Phys. Lipids* 2008. **153**:57-63, 2008.
- [12] N. V. Eldho, S. E. Feller, S. Tristram-Nagle, I. V. Polozov, K. Gawrisch, *J. Am.*

- Chem. Soc.* 125:6409-6421, 2003.
- [13] S. Basinger, D. Bok and M. Hall, *J. Cell. Biol.* 69:29-42, 1976.
- [14] K. Gawrisch, O. Soubias and M. Mihailescu, *Prostaglandins Leukot Essent Fatty Acids*, 79: 131-134, 2008.
- [15] M. I. Aveldano, *J. Biol. Chem.* 262:1172-1179, 1987.
- [16] M. I. Aveldano and H. Sprecher, *J. Biol. Chem.* 262:1180-1186, 1987.
- [17] M-P. Agbaga, M. N. A. Mandal and R.E. Anderson, *J. Lipid Res.* 51:1624-1642, 2010.
- [18] E. Lindahl, B. Hess and D. van der Spoel, *J. Mol. Mod.* 7:306-317, 2001.
- [19] W. F. van Gunsteren, S. R. Billeter, A. A. Eising, P.H. Hünenberger, P. Krüger, A. E. Mark, W. R. P. Scott, and I. G. Tironi, *Biomolecular simulation: The GROMOS96 Manual and user guide*. Vdf Hochschulverlag AG an der ETH Zürich, Zürich, Switzerland, 1996.
- [20] H. J. C. Berendsen, J. P. M. Postma, W. F. van Gunsteren, A. DiNola, and J. R. Haak, *J. Chem. Phys.* 81:3684-3690, 1984.
- [21] T. Darden, D. York and L. Pedersen, *J. Chem. Phys.* 98:10089-10092, 1993.
- [22] U. Essmann, L. Perera, M. L. Berkowitz, T. Darden, H. Lee and L. G. Pedersen,

*J. Chem. Phys.* 103:8577-8593, 1995.

[23] T. Kobayashi, *LipidBank: Clupanodonic acid*. 2010 [cited 2010 31 August];

Available from: <http://lipidbank.jp/cgi-bin/detail.cgi?id=DFA0222>.

[24] T. Farkas, K. Kitajka, E. Fodor, I. Csengeri, E. Lahdes, Y. K. Yeo, Z. Krasznai, and J. E. Halver, *Proc. Natl. Acad. Sci. U S A* 97:6362-6366, 2000.

[25] I. Dey, C. Buda, T. Wiik, J. E. Halver, and T. Farkas, *Proc. Natl. Acad. Sci. U S A* 90:7498-7502, 1993.

[26] T. Kaneda, *Microbiol Rev.* 55:288-302, 1991.

[27] D. F. Silbert, R. C. Ladenson and J. L. Honegger, *Biochim. Biophys. Acta* 311:349-61, 1973.

[28] A. D. Purdon and S.I. Rapoport, *4.6 Energy Consumption by Phospholipid Metabolism in Mammalian Brain*, in *Neural Energy Utilization: Handbook of Neurochemistry and Molecular Biology*, G. Gibson and G. Dienel, Editors. 2007, Springer: New York. p. 401-427.